Canonical studies of the cluster distribution, dynamical evolution, and critical temperature in nuclear multifragmentation processes

S. J. Lee*
Department of Physics and Astronomy, Rutgers University, Piscataway, New Jersey 08855

A. Z. Mekjian†
Institute of Nuclear Theory, HN-12, University of Washington, Seattle, Washington 98195
(Received 6 May 1991)

Partition functions for a canonical and microcanonical ensemble are developed which are then used to describe various properties of excited hadronic systems. Relating multinomial coefficients to a generating function of these partition functions, it is shown that the average value of various moments of cluster sizes are of a quite simple form in terms of canonical partition functions. Specific applications of the results are to partitioning problems as in the partitioning of nucleons into clusters arising from a nuclear collision and to branching processes as in Furry branching. The underlying dynamical evolution of a system is studied by parametrizing the multinomial variables of the theory. A Fokker-Planck equation can be obtained from these evolutionary equations. By relating the parameters and variables of the theory to thermodynamic variables, the thermal properties of excited hadronic systems are studied.

PACS number(s): 25.70.Pq, 24.60.−k, 05.70.−a, 05.40.+j

I. INTRODUCTION

Nuclear systems under various amounts of excitation show a wide variety of different behavior. At low excitation energy, single particle and collective excitations such as giant resonances are seen. Gamma emission, evaporation of a nucleon, and fission are possible simple modes of decay. As the excitation energy increases, more complex decay schemes manifest themselves. The nuclear system fragments into more pieces as this energy is increased. The region where the excitation energy is near to the binding energy is of current interest. This region is called the multifragmentation region. Within this region lie the possibility of seeing a liquid-gas phase transition in the nuclear matter limit, i.e., in an infinitely large nuclear system. At still higher energies, particles such as pions and kaons can be produced. At very high energies, a quark-gluon phase may be reached. When particles are produced or a transition is made to the quark-gluon plasma, new degrees of freedom are created. In the multifragmentation region, the initial number of baryons are redistributed into clusters of various sizes and into single nucleons. How nucleons in a nuclear system at moderate excitation energy are redistributed among clusters, and how the initial excitation energy affects the modes of decay, will be studied here. This paper is a continuation of work started in Refs. [1,2].

Except in infinite nuclear matter, the number of nucleons in a nuclear system is too small to be considered as a thermodynamic system. Only up to few hundred nucleons are involved in a heavy-ion collision. Thus the study of nuclear multifragmentation phenomena requires nonequilibrium considerations and fluctuation studies due to the finiteness of the system. The large number limit of this study should lead to thermodynamic phenomena such as the liquid-gas phase transition, critical phenomena, and the spinodal instability. Our study here considers the modes at the final state of a nuclear system after experiencing a dynamical instability such as a spinodal instability.

An outline of this paper is as follows. Section II contains a framework for investigating the partitioning of a nucleus into clusters. A general grand canonical partition function is developed in terms of multinomials. Then canonical and microcanonical partition functions are developed from this grand canonical partition function. The distribution of cluster sizes is then developed and fluctuations are studied. Section III investigates the underlying dynamical evolution of the cluster size distribution function. In Secs. II and III, very general formulations are considered. One special case of these formulations is related to nuclear fragmentation phenomena. Section IV shows how the excitation energy controls the distribution of fragments. The various special temperatures of a nuclear system are also discussed. Section V is for concluding remarks and some detail derivations are given in the appendixes.

II. GENERALIZED PARTITION FUNCTIONS, DISTRIBUTIONS, AND FRAGMENTATION PROCESSES

A method for investigating the fragmentation of a nuclear system into clusters of nucleons will be developed. The partitioning of A initial nucleons into groups of varying sizes gives rise to a distribution of cluster sizes.

*Electronic address: sjlee@ruthep.rutgers.edu.
†Permanent address: Dept. of Physics and Astronomy, Rutgers University, Piscataway, NJ 08855. Electronic address: mekjian@ruthep.rutgers.edu.

Let n_k be the number of clusters of size k. The n_1 is then the number of nucleons not in clusters. A partition

$$\mathbf{n}=\{n_i\}=(n_1,n_2,n_3,\ldots,n_A) \tag{1}$$

defines a particular arrangement of the initial nucleons into clusters $(n_2,n_3,\ldots,n_A)$ and monomers (n_1) regardless of which nucleon belongs to which cluster. A constraint exists which is

$$A=\sum_{i=1}^{A} in_i \ . \tag{2}$$

The number of clusters in a particular partition is called the multiplicity M,

$$M=\sum_{i=1}^{A} n_i \ . \tag{3}$$

The counting of partitions for a given A can be related to the partition of an integer A into a summand of smaller integers without regard to order [1,3]. This counting and its generating function are discussed in Sec. II B together with other types of counting.

Each partition $\mathbf{n}$ is then assigned a weight. Ensemble averages over all possible fragmentation partitions can be carried out using this weight. For example, Ref. [1] considered a weight which is simply

$$W_A(\mathbf{n},x)=M_2(A,\mathbf{n})x^M \ , \tag{4}$$

where M_2 is a Cauchy's number [4]

$$M_2(A,\mathbf{n})=\frac{A!}{\prod_{j=1}^{A} j^{n_j}n_j!}=\frac{A!}{1^{n_1}n_1!2^{n_2}n_2!\cdots A^{n_A}n_A!} \ . \tag{5}$$

The x is an evolutionary tuning parameter discussed in Refs. [1,2]. While M_2 contains combinatoric factors, the x contains the underlying physical quantities which determine the distribution of cluster sizes. References [1] and [3] relate x to the freeze out volume and freeze out temperature, to the binding energy per particle, and to the level density. Section IV contains a discussion of x which can vary from zero to infinity. As x increases, the weighting factor x^M in Eq. (4) shifts the fragmentation scheme from low multiplicity to high multiplicity events. The $M=2$ modes of decay correspond to the system breaking into two pieces, the $M=3$ modes correspond to a fragmentation into three pieces, etc. At $x=0$, only one cluster made of all nucleons exists and at $x=\infty$, the fragmentation results in A nucleons. In between these two extremes, we have all other possibilities. For example, for small x the mode of decay can be evaporation of a particle from a heated system while for large x, the system will break up into many nucleons and some small clusters.

Once a weight function, $W_A(\mathbf{n},x)$, is assigned to each partition $\mathbf{n}$, a canonical ensemble partition function can be obtained from

$$Q_A(x)=\sum_{\{n_i\}}\delta\left[\sum_i in_i-A\right]W_A(\mathbf{n},x) \ , \tag{6}$$

where the sum is over all possible values of n_i's, i.e.,

$$\sum_{\{n_i\}}=\sum_{n_1=0}^{\infty}\sum_{n_2=0}^{\infty}\cdots\sum_{n_i=0}^{\infty}\cdots\sum_{n_N=0}^{\infty} \ . \tag{7}$$

The constraint $A=\sum_i in_i$ of Eq. (2) is represented by the delta function $\delta(n)$ in Eq. (6); $\delta(n)=\delta_{n,0}$ for a discrete argument. For the $W_A(\mathbf{n},x)$ given by Eq. (4), the $Q_A(x)$ of Eq. (6) can be generated by an exponential generating function [1,2,3]

$$Q(u,x)=\sum_{A=0}^{\infty}Q_A(x)\frac{u^A}{A!}=\exp\left[\sum_{i=1}^{\infty}x\frac{u^i}{i}\right]=\left[\frac{1}{1-u}\right]^x \ . \tag{8}$$

Thus we have

$$Q_A(x)=x(x+1)(x+2)\cdots(x+A-1)=\frac{\Gamma(x+A)}{\Gamma(x)} \ . \tag{9}$$

The $\Gamma(x)$ is the gamma function which is $(x-1)!$ if x is an integer.

Properties of the cluster size distribution function resulting from Eq. (9) can be found in Refs. [1,2,3]. The mean number of clusters of size i obtained from

$$Y_A(k,x)=\frac{\sum_{\{n_i\}}\delta\left[\sum_i in_i-A\right]n_kW_A(\mathbf{n},x)}{Q_A(x)} \tag{10}$$

in a canonical ensemble is simply

$$Y_A(k,x)=\binom{A}{k}xB(x+A-k,k) \ . \tag{11}$$

Here $\binom{A}{k}=A!/k!(A-k)!$ and $B(x+A-k,k)=\Gamma(x+A-k)\Gamma(k)/\Gamma(x+A)$ are the binomial coefficient and the beta function, respectively. For large A and $k\ll A$,

$$Y_A(k,x)\approx\frac{x}{k}e^{-\lambda k} \ , \tag{12}$$

where the Lagrange multiplier λ is determined by $\sum_k kY_A(k,x)=A$. This Maxwell-Boltzmann-like distribution is a special case of the more general expression studied in Ref. [2]. If no microcounting factor or evolutionary tuning parameter is included, i.e., putting $W_A(\mathbf{n},x)=1$ in Eq. (6), then the yield $Y_A(k)$ for a large A is simply

$$Y_A(k)\approx\frac{1}{4\sqrt{3}A}\frac{1}{\exp[(\pi/2)k\sqrt{2/(3A)}]-1} \ , \tag{13}$$

which is the Bose-Einstein-like distribution obtained in Ref. [5]. The effect of the finiteness of A in Bose-Einstein statistics is studied in Ref. [6] and the corresponding number of partitions are discussed in Sec. II B.

We will generalize the partition function of Eq. (8) in Sec. II A. In Sec. II B, we discuss the relations with various partitions of an integer. Section II C relates the partition functions to the mean and various moments of the distribution in a canonical ensemble. Finally, the various factorial moments in a microcanonical ensemble are considered in Sec. II D.

A. Generalized partition functions

We now extend Eq. (8) by considering a more general generating function of the form

$$Q(u,\mathbf{x})=\exp\left[\sum_{i=1}^{N}\frac{1}{\beta_i}x_i u^{\alpha_i}\right]=\sum_{M=0}^{\infty}\frac{1}{M!}\left[\sum_{i=1}^{N}\frac{u^{\alpha_i}}{\beta_i}x_i\right]^M, \quad (14)$$

which is an infinite sum of multinomials. The $\mathbf{x}=\{x_i\}=(x_1,x_2,\ldots,x_N)$ is the set of N multinomial variables. Each cluster i has an x_i associated with it. The case $\alpha_i=\beta_i=i$ with all the x_i's equal to a single x is then Eq. (8). The grand canonical partition function $Q(u,\mathbf{x})$ generates the canonical partition function $Q_A(\mathbf{x})$ through the relation of

$$Q(u,\mathbf{x})=\sum_A Q_A(\mathbf{x})\frac{u^A}{\Gamma(A+1)}=\sum_{\{n_i\}}G_A(\mathbf{n},\mathbf{x})\frac{u^A}{\Gamma(A+1)}. \quad (15)$$

The sum over $\{n_i\}$ is given by Eq. (7) and the sum over A is for all possible values of A given by

$$A=\sum_{i=1}^{N}\alpha_i n_i . \quad (16)$$

Here A may have any value depending on the α_i. However, if we restrict α_i to $\alpha_i=i$ as in a nuclear fragmentation, only the integer values are allowed for A and Eq. (16) reduces to Eq. (2). For this case we have $\Gamma(A+1)=A!$. The $G_A(\mathbf{n},\mathbf{x})$ is the weight function of a specific partition $\mathbf{n}$ of A into a summand of α_i's and is given by

$$G_A(\mathbf{n},\mathbf{x})=\frac{\Gamma(A+1)}{M!}C(M,\mathbf{n})\prod_{i=1}^{N}\left[\frac{x_i}{\beta_i}\right]^{n_i}=\Gamma(A+1)\prod_{i=1}^{N}\left[\frac{x_i^{n_i}}{\beta_i^{n_i}n_i!}\right], \quad (17)$$

where

$$C(M,\mathbf{n})=\frac{M!}{\prod_{j=1}^{N}n_j!}=\frac{M!}{n_1!n_2!\cdots n_N!}. \quad (18)$$

The multiplicity M is given by Eq. (3) and the $C(M,\mathbf{n})$ is the multinomial coefficient of the term specified by $\mathbf{n}$ in the expansion of the Mth order multinomial. The $G_A(\mathbf{n},\mathbf{x})$ of Eq. (17) reduces to the weight function $W_A(\mathbf{n},x)$ of Eq. (4) when $\alpha_i=\beta_i=i$ and $x_i=x$. The summation over M in Eq. (14) results in the connection between the multinomial factor and the grand canonical partition function $Q(u,\mathbf{x})$ which is the generating function of the canonical partition function $Q_A(\mathbf{x})$ for fixed A. Cole [7] has considered a multinomial expansion without the summation over M and thus has a generating function for a microcanonical partition function for fixed A and M instead of a generating function for a canonical partition function. We will also give results for an exactly soluble microcanonical ensemble in Sec. II D.

Before going further, let us define a shorter notation for various summations:

$$\sum_{\{n_i\}_A}=\sum_{\{n_i\}}\delta\left[\sum_{i=1}^{N}\alpha_i n_i-A\right],$$

$$\sum_{\{n_i\}_{A,M}}=\sum_{\{n_i\}}\delta\left[\sum_{i=1}^{N}\alpha_i n_i-A\right]\delta\left[\sum_{i=1}^{N}n_i-M\right], \quad (19)$$

$$\sum_{\{n_i\}_{A,n_k'}}=\sum_{\{n_i\}}\delta\left[\sum_{i=1}^{N}\alpha_i n_i-A\right]\delta(n_k-n_k'),$$

i.e., constrained summations of Eq. (7) with the fixed values of $\sum_i\alpha_i n_i=A$, $\sum_i\alpha_i n_i=A$, and $\sum_i n_i=M$, and $\sum_i\alpha_i n_i=A$ and $n_k=n_k'$, respectively. With these notations, the unconstrained summation of Eq. (7) can be expressed by

$$\sum_{\{n_i\}}=\sum_A\sum_{\{n_i\}_A}=\sum_A\sum_M\sum_{\{n_i\}_{A,M}}=\sum_A\sum_{n_k'}\sum_{\{n_i\}_{A,n_k'}}. \quad (20)$$

The canonical partition function then becomes, from Eq. (15),

$$Q_A(\mathbf{x})=\left[\left[\frac{d}{du}\right]^A Q(u,\mathbf{x})\right]_{u=0}=\sum_{\{n_i\}_A}G_A(\mathbf{n},\mathbf{x})=\sum_{\{n_i\}_A}\Gamma(A+1)\prod_{i=1}^{N}\left[\frac{x_i^{n_i}}{\beta_i^{n_i}n_i!}\right]. \quad (21)$$

Except for the differential representation $(d/du)^A$, the expression in Eq. (21) applies to the case with arbitrary values of α_i. We also define the following quantities:

$$Q_A^M(\mathbf{x})=\sum_{\{n_i\}_{A,M}}G_A(\mathbf{n},\mathbf{x})=\sum_{\{n_i\}_{A,M}}\Gamma(A+1)\prod_{i=1}^{N}\left[\frac{x_i^{n_i}}{\beta_i^{n_i}n_i!}\right], \quad (22)$$

$$Q_A^{n_k}(\mathbf{x})=\sum_{\{n_i\}_{A,n_k}}G_A(\mathbf{n},\mathbf{x})=\sum_{\{n_i\}_{A,n_k}}\Gamma(A+1)\prod_{i=1}^{N}\left[\frac{x_i^{n_i}}{\beta_i^{n_i}n_i!}\right]. \quad (23)$$

The $Q_A^M(\mathbf{x})$ and $Q_A^{n_k}(\mathbf{x})$ can be nonzero only for $A\geq 0$ for the case $\alpha_i=i$. The $Q_A^M(\mathbf{x})$ and $Q_A^{n_k}(\mathbf{x})$ are more constrained than the canonical partition function $Q_A(\mathbf{x})$ and

$$Q_A(\mathbf{x})=\sum_{M=0}^{\infty}Q_A^M(\mathbf{x})=\sum_{n_k=0}^{\infty}Q_A^{n_k}(\mathbf{x}). \quad (24)$$

Considering $x_i\to x_i t$ in Q_A, Q_A^M can be found using Q_A as

$$Q_A^M(\mathbf{x})=\frac{1}{M!}\left[\left[\frac{d}{dt}\right]^M Q_A(t\mathbf{x})\right]_{t=0} . \tag{25}$$

Here, $Q_A^M(\mathbf{x})$ and $Q_A^{n_k}(\mathbf{x})$ can be considered microcanonical partition functions in the sense that they are more constrained than the canonical partition function $Q_A(\mathbf{x})$. For a system which has total energy proportional to the multiplicity M [see Eq. (85) in Sec. IV], $Q_A^M(\mathbf{x})$ becomes the usual microcanonical partition function in thermodynamics, i.e., partition function for fixed energy. The various partition functions for the $\alpha_i=\beta_i=1$ case and the $\alpha_i=\beta_i=i$ case are given in Appendixes A and B, respectively.

In Eqs. (14)–(25), the α_i's and β_i's may, in general, have any value. All the following discussions in Secs. II and III are applicable for general α_i and β_i unless it is explicitly specified. However, for simplicity, only positive integer values of α_i are considered. The A is then a nonnegative integer and $Q_A(\mathbf{x})=0$ for $A<0$. Here $A=0$ only when all the n_i's are zero and $Q_0(\mathbf{x})=1$. Otherwise, A is a positive integer. We will also use $A!$ instead of $\Gamma(A+1)$. When $\alpha_i=i$, the species i is represented as a cluster with the size specified in terms of the number of constituents. Then $A=\sum_i \alpha_i n_i=\sum_i i n_i$ is the total number of nucleons in the fragmentation of a nucleus into clusters with any size between 1 and A.

As can be seen from Eqs. (15) and (21)–(23), partition functions depend solely on the weight function $G_A(\mathbf{n},\mathbf{x})$ beside the obvious constraints on A and M. Equation (17) shows that various factors are involved in determining the weight $G_A(\mathbf{n},\mathbf{x})$: The parameter x_i, which represents the characteristics of each species or cluster i, may be related to an evolution parameter as will be discussed in Sec. III or to thermodynamic quantities as will be discussed in Sec. IV in more detail. Section II B contains a discussion of the n_i dependence of $G_A(\mathbf{n},\mathbf{x})$ and illustrates other types of microstate counting rules. Finally, the parameters α_i and β_i characterize the structure of species i which we will discuss in the rest of this subsection.

The physical system considered specifies the choice to be taken for quantities α_i's and β_i's. Here we discuss various physical situations for the choice of these quantities. If we consider nuclear fragmentation described by the number of nucleons in a cluster with a fixed total number of nucleons A, then $\alpha_i=i$ are positive integers from 1 to A with i the size of the cluster. If we consider a system of baryons and antibaryons with fixed total baryon number A, α_i are positive and negative integers which are unbound and can even be larger than A. On the other hand, we may relate α_i with the energy of a single particle level in a nucleus or of an oscillator. Then A corresponds to the total energy which is the sum of those level energies. Identifying α_i as the spin of the species i, which is an integer or a half integer, A becomes the total spin of the system. If we consider hadrons as the colorless realization of a quark-antiquark system, the existing α_i's are 2 for mesons, 3 for baryons, and 6 for dibaryons. For the case of clusters with even number of elements only, which is studied in Ref. [3] and may be applicable to various pairing phenomena, $\alpha_i=i$ for even i and no species i exists for odd i. As we can see from Eqs. (16) and (17), the nonexistence of some species i can be represented by either $\alpha_i=\infty$, $\beta_i=\infty$, or $x_i=0$ for the corresponding i. With the choice of $\alpha_i=\beta_i=1$, we may study branching phenomena such as jet fragmentation in ϕ^3 theory [8] having $N+1=3$ lines at each vertex [see Eq. (61) in the next section]. For this case, the $N=2$ is the number of branches per each stem in a tree diagram. The case with $\alpha_i=\beta_i=i$ and $N=\infty$ is the generalization of Eq. (9) with general x_i. This choice applies to the nuclear fragmentation process of the total A nucleons into n_i clusters with i nucleons. Equations (8) and (9) are the one parameter case of $x_i=x$. The two parameter case with $x_i=xy^{\delta_{i,1}}$ is studied in Ref. [2] (see Appendix B). We also study other various choices of x_i's in Ref. [3] which also are exactly soluble.

The β_i may be related to the number of rearrangements of constituents in a cluster i (see discussion in Sec. II B). If we consider a cycle in a permutation [3], $\beta_i=i$ for a cycle of length i, and $\beta_i=i!$ if we consider a cluster constituted with i classical particles. The Cauchy's number of Eq. (5) corresponds to $G_A(\mathbf{n},\mathbf{x})$ of Eq. (17) with $\alpha_i=\beta_i=i$ and $x_i=1$ for $i\le N=A$. For this case, the canonical partition function $Q_A(\{x_i=1\})$ becomes the total number of possible partitions of A particles into different sizes of cycles in Maxwell-Boltzmann statistics [see Eq. (31) in Sec. II B]. For $x_i=x$, $Q_A(\mathbf{x})$ becomes $Q_A(x)$ of Eq. (9). Particle rearrangements are allowed in this partition through the factor $\Gamma(A+1)=A!$ in the weighting function $G_A(\mathbf{n},\mathbf{x})$ of Eq. (17) together with the multinomial coefficient $C(M,\mathbf{n})$ of Eq. (18). Furthermore, the particle rearrangements in a cluster can also be considered through proper choice of β_i. Thus this model of Eqs. (14)–(18) is proper in describing the fragmentation of participating nucleons after thermal equilibration. In contrast to this case, Eq. (13) or the $p_{\mathrm{BE}}(A)$ discussed in Sec. II B does not allow for any rearrangement of nucleons and thus can describe only a prompt fragmentation process before reaching thermal equilibrium.

B. Partitions of integer and generating functions

In this subsection we compare various possible choices of the microcounting factors appearing in the weight function $W_A(\mathbf{n},x)$ of Eq. (4) or $G_A(\mathbf{n},\mathbf{x})$ of Eq. (17). Clusterization of A elements can be related with a partition of an integer A into a summand of smaller integers. A specific microstate counting rule determines the structure of the weight function.

Sobotka and Moretto [6] have shown that the decomposition of an integer A into integer summands $A=\sum_i i n_i$ [Eq. (2)] without regard to order can approximate the fragmentation of a nucleus of size A through nucleon-nucleus collision. The number of such partitions of A is called $p_{\mathrm{BE}}(A)$ where the subscript BE just indicates that the counting of the partitions follows Bose-Einstein (BE) like rules; same integer can appear several times in a partition without regard to order. Such decomposition of an integer A into n_1 of 1's, n_2 of 2's, . . ., and n_A of A's is represented by a partition $\mathbf{n}$ of Eq. (1), and the total number of these decompositions can be represented by

$$p_{\rm BE}(A)=\sum_{\{n_i\}}\delta\left[\sum_i in_i-A\right]=\sum_{\{n_i\}_A}1\ . \qquad (26)$$

Here the summations are defined by Eqs. (7) and (19). This $p_{\rm BE}(A)$ is the same as the canonical partition function Q_A of Eq. (6) with $W_A(\mathbf{n},x)=1$. For $A=3$, as an example, $p_{\rm BE}(3)=3$ with the partitions of $3=2+1=1+1+1$. Here, partitions are, in terms of $\mathbf{n}$ of Eq. (1), $\mathbf{n}=(0,0,1)$ for the partition 3, $\mathbf{n}=(1,1,0)$ for the partition $2+1$, and $\mathbf{n}=(3,0,0)$ for the partition $1+1+1$. Minimal information or maximum entropy consideration, which treats each partition with the same weight $[W_A(\mathbf{n},x)=1$ or put $G_A(\mathbf{n},x)=1$ in Eq. (21)], determines the size distribution in a nuclear fragmentation process [6]. The large A limit of this partition gives the Bose-Einstein-like distribution Eq. (13) obtained by Aichelin and Huefner [5] in their description of fragmentation. Due to the BE counting rule for clusters without any rearrangement of their constituent nucleons, this model may describe the distribution of fragments broken off through the prompt fragmentation of a nucleus in a nucleon-nucleus collision or from the most unstable (excited) part of the spectator in heavy-ion collisions before its thermal equilibration. This corresponds to approximating a nuclear fragmentation as a shattering of a glass ball through bombarding with a small projectile.

If we distinguish all the different orders of integers, we need to consider the rearrangement of integers in a specific partition. This rearrangement gives rise to a microstate counting factor for each partition $\mathbf{n}=\{n_i\}$ which is the corresponding multinomial coefficient $C(M,\mathbf{n})$ of Eq. (18):

$$(x_1+x_2+\cdots+x_N)^M=\sum_{\{n_i\}_M}C(M,\mathbf{n})x_1^{n_1}x_2^{n_2}\cdots x_N^{n_N}\ . \qquad (27)$$

The M is the multiplicity (the total number of integers) for the partition $\mathbf{n}$ and is given by Eq. (3). The $n_j!$'s in the denominator of $C(M,\mathbf{n})$ are the Gibbs factorials arising from the indistinguishability of the same integers in the Maxwell-Boltzmann (MB) statistics for M integers. Here each integer can be assigned a distinguishable position in contrast to the Bose-Einstein case in which all the integers appear at indistinguishable points. Weighting each partition by $C(M,\mathbf{n})$, we have

$$p_{\rm MB}(A)=\sum_{\{n_i\}}\delta\left[\sum_i in_i-A\right]C(M,\mathbf{n})=\sum_{\{n_i\}_A}C(M,\mathbf{n})\ . \qquad (28)$$

This corresponds to the number of partitions of an integer A into integer summands distinguishing different orders, i.e., counting the partitions with MB statistics for clusters. This $p_{\rm MB}(A)$ also can be considered as the number of possible cuts in the $(A-1)$ links for A serial points, thus $p_{\rm MB}(A)=2^{A-1}$. For example, $p_{\rm MB}(3)=4$ with $3=2+1=1+2=1+1+1$. The corresponding partitions are one of $\mathbf{n}=(0,0,1)$, two of $\mathbf{n}=(1,1,0)$, and one of $\mathbf{n}=(3,0,0)$. The $p_{\rm MB}(A)$ of Eq. (28) can be considered as a canonical partition function Q_A of Eq. (6) with the weighting factor $W_A(\mathbf{n},x)=C(M,\mathbf{n})$, or Q_A of Eq. (21) with the weighting function $G_A(\mathbf{n},\mathbf{x})=C(M,\mathbf{n})$. Due to the Maxwell-Boltzmann counting rule for clusters without any rearrangement of their constituent nucleons, this partition function may describe a shattering of a glass ball through colliding with another large ball or a prompt fragmentation (through cracking) of the participants in heavy-ion collisions before its thermal equilibration.

Similarly, we can consider Fermi-Dirac (FD) rules in counting the clusters (integers), i.e., allow only zero or one cluster for each size; $n_i\le 1$. In this case, the number of partitions of an integer A into distinct integer summands without regard to order becomes

$$p_{\rm FD}(A)=\sum_{\{n_i\}}\delta\left[\sum_i in_i-A\right]\prod_i[\delta(n_i)+\delta(n_i-1)]$$
$$=\sum_{\{n_i\}_A}\prod_i[\delta(n_i)+\delta(n_i-1)]\ . \qquad (29)$$

For example, $p_{\rm FD}(3)=2$ with $3=2+1$ where the partitions are 3 which is $\mathbf{n}=(0,0,1)$ and $2+1$ which is $\mathbf{n}=(1,1,0)$. The partition $\mathbf{n}=(3,0,0)$, which is $1+1+1$, is not allowed here. The $p_{\rm FD}(A)$ corresponds to a canonical partition function Q_A of Eq. (21) with the weighting function $G_A(\mathbf{n},\mathbf{x})=\prod_i[\delta(n_i)+\delta(n_i-1)]$. Due to this restriction on the allowed values of n_i, this partition may be connected with some special case of a sandpile problem [3,9].

The generating functions [4] for $p_{\rm FD}(n)$, $p_{\rm BE}(n)$, and $p_{\rm MB}(n)$ are

$$\sum_{n=0}^{\infty}p_{\rm FD}(n)u^n=\prod_{i=1}^{\infty}(1+u^i)\ ,$$
$$\sum_{n=0}^{\infty}p_{\rm BE}(n)u^n=\prod_{i=1}^{\infty}(1-u^i)^{-1}\ , \qquad (30)$$
$$\sum_{n=0}^{\infty}p_{\rm MB}(n)u^n=\sum_{m=0}^{\infty}\left[\sum_{i=1}^{\infty}u^i\right]^m$$
$$=\left[1-\left[\sum_{i=1}^{\infty}u^i\right]\right]^{-1}=\frac{(1-u)}{(1-2u)}\ .$$

All of these are polynomial generating functions. By contrast, $Q_A(x)$ of Eq. (21) has an exponential generating function given by Eq. (14).

Since it does not allow any rearrangement of nucleons and counts partitions without regard to order, the $p_{\rm BE}(A)$ may be applicable to the fragmentations of spectators in heavy-ion collisions or nucleon-nucleus collisions in which some clusters break off from the most unstable (excited) part of the system before its thermal equilibration. The different order of clusters, which is considered in the $p_{\rm MB}(A)$, corresponds to the breakup of a nucleus at a different place. The Maxwell-Boltzmann statistics may describe prompt fragmentation of the participants in a heavy-ion collision. However, both of these

$p_{\mathrm{BE}}(A)$ and $p_{\mathrm{MB}}(A)$ do not allow for any rearrangement of nucleons. They thus consider clusters without regard to their internal nucleonic structure. Due to the neglect of nucleon rearrangements in the system, these partitions may only be applicable to prompt fragmentation (through cracking) before thermal equilibration in a fashion similar to the shattering of a glass ball.

To consider the rearrangement of constituents in the system, we need to replace the multinomial coefficients $C(M,\mathbf{n})$ in $p_{\mathrm{MB}}(A)$ of Eq. (28) by $(A!/M!)C(M,\mathbf{n})=A!/n_1!n_2!\cdots n_N!$. The factor $A!$ counts the rearrangements of A nucleons; the factor $M!$ in $C(M,\mathbf{n})$ counts the rearrangements of M clusters but not nucleons. However using $A!$ instead of $M!$ overcounts due to the indistinguishability among clusters of the same size: We need to consider the rearrangement of nucleons in a cluster such as the Gibbs factorial, $i!$. Representing the number of rearrangements of nucleons in a cluster i by β_i, we have the weighting function $G_A(\mathbf{n},\mathbf{x})$ of Eq. (17). The partition of an integer A [here, $\alpha_i=i$ in Eq. (16)] with this weight factor for each partition gives rise to a canonical partition function given by Eq. (21). This canonical partition function has an exponential generating function of Eq. (14) which is the sum of multinomials Eq. (27) of all order. The specific choice of $\beta_i=i$, which represents cyclic rearrangement of i components, weights each partition $\mathbf{n}$ by a corresponding Cauchy's number $M_2(A,\mathbf{n})$ of Eq. (5) and gives various exactly soluble models [1,2,3] such as the case given by Eq. (9).

The Cauchy's number $M_2(A,\mathbf{n})$ of Eq. (5) corresponds to $G_A(\mathbf{n},\mathbf{x})$ of Eq. (17) with $\alpha_i=\beta_i=i$ and $x_i=1$ for $i\le N=A$. For this case, the sum of partitions of an integer A with weighting factor $M_2(A,\mathbf{n})$ gives the partition function $Q_A(1)$ given by Eq. (6) or (9) with $x=1$,

$$Q_A(1)=\sum_{\{n_i\}}\delta\left[\sum_i in_i-A\right]M_2(A,\mathbf{n})=\sum_{\{n_i\}_A}M_2(A,\mathbf{n})=A!\ . \tag{31}$$

The particle rearrangements are allowed in these partitions in contrast to the previous ones [$p_{\mathrm{MB}}(A)$, $p_{\mathrm{BE}}(A)$, and $p_{\mathrm{FD}}(A)$]. Furthermore, the particle rearrangements in a cluster are also considered through proper choice of β_i. Thus this is more proper in describing the fragmentation of participants after thermal equilibration, i.e., after the system reaches a uniform distribution. Notice that the $Q_A(1)$ of Eq. (31) is a MB distribution of A constituent particles (nucleons) in contrast to the $p_{\mathrm{MB}}(A)$ of Eq. (28) which is a MB distribution of M clusters without any rearrangement of their constituent nucleons. For example, $Q_3(1)=6$ with one of partition $\mathbf{n}=(3,0,0)$, three of partition $\mathbf{n}=(1,1,0)$, and two of partition $\mathbf{n}=(0,0,1)$. The least information principle in this MB statistics of A nucleons determines the cluster size distribution given by $1/k$ which is a special case of Eq. (11) with $x=1$.

C. Canonical ensemble averages

This subsection illustrates how to use the partition function to obtain canonical ensemble averages of various quantities of interest. Various derivatives of Eqs. (15)–(23) with respect to x_i are of interest since these derivatives give information about the distribution of cluster sizes. As an example, the derivatives of Eq. (17) lead to

$$\left[x_j\frac{d}{dx_j}\right]^l\left[x_k\frac{d}{dx_k}\right]^m G_A(\mathbf{n},\mathbf{x})=n_j^l n_k^m G_A(\mathbf{n},\mathbf{x})\ , \tag{32}$$

$$[x_j]^l[x_k]^m\left[\frac{d}{dx_j}\right]^l\left[\frac{d}{dx_k}\right]^m G_A(\mathbf{n},\mathbf{x})=\frac{n_j!}{(n_j-l)!}\frac{n_k!}{(n_k-m)!}G_A(\mathbf{n},\mathbf{x})\ . \tag{33}$$

Notice that Eq. (32) becomes zero only when n_j or n_k is zero in contrast to Eq. (33) which is nonzero only when $l\le n_j$ and $m\le n_k$. Equation (33) also applies to the case of $j=k$ with $n_j=(n_k-m)$, i.e., replacing the factorial factors on the right-hand side by $n_k!/(n_k-m-l)!$. Then factorial moments are contained in a function

$$F^{n_k}_{A,m}(\mathbf{x})=[x_k]^m\left[\frac{d}{dx_k}\right]^m Q^{n_k}_A(\mathbf{x})=\sum_{\{n_i\}_{A,n_k}}\frac{n_k!}{(n_k-m)!}G_A(\mathbf{n},\mathbf{x})=\frac{n_k!}{(n_k-m)!}Q^{n_k}_A(\mathbf{x})\ , \tag{34}$$

for $m\le n_k$. The correlations between different factorial moments are contained in the derivative of the canonical partition function $Q_A(\mathbf{x})$;

$$[x_j]^l[x_k]^m\left[\frac{d}{dx_j}\right]^l\left[\frac{d}{dx_k}\right]^m Q_A(\mathbf{x})=\sum_{\{n_i\}_A}\frac{n_j!}{(n_j-l)!}\frac{n_k!}{(n_k-m)!}G_A(\mathbf{n},\mathbf{x})\ , \tag{35}$$

for $m\le n_k$ and $l\le n_j$. Using Eq. (17) for $G_A(\mathbf{n},\mathbf{x})$ and the fact that

$$\delta\left[\sum_{i=1}^N\alpha_i n_i-A\right]=\delta\left[\left[\sum_{i\ne k}^N\alpha_i n_i+\alpha_k n_k'\right]-(A-m\alpha_k)\right] \tag{36}$$

for $n_k'=n_k-m$, we can show that

$$F^{n_k}_{A,m}(\mathbf{x})=\left[\frac{x_k}{\beta_k}\right]^m \frac{A!}{(A-m\alpha_k)!}Q^{(n_k-m)}_{(A-m\alpha_k)}(\mathbf{x}) , \tag{37}$$

$$[x_j]^l[x_k]^m\left[\frac{d}{dx_j}\right]^l\left[\frac{d}{dx_k}\right]^m Q_A(\mathbf{x})=\left[\frac{x_j}{\beta_j}\right]^l\left[\frac{x_k}{\beta_k}\right]^m\frac{A!}{(A-l\alpha_j-m\alpha_k)!}Q_{(A-l\alpha_j-m\alpha_k)}(\mathbf{x}) . \tag{38}$$

Here $m\le n_k$ and $(A-m\alpha_k)\ge 0$ for $F^{n_k}_{A,m}$ of Eq. (37), and $(A-l\alpha_j-m\alpha_k)\ge 0$ for Eq. (38). Moreover,

$$\begin{aligned}[x_j]^l\left[\frac{d}{dx_j}\right]^l F^{n_k}_{A,m}(\mathbf{x})&=\sum_{\{n_i\}_{A,n_k}}\frac{n_k!}{(n_k-m)!}\frac{n_j!}{(n_j-l)!}G_A(\mathbf{n},\mathbf{x})\\&=\frac{A!}{(A-l\alpha_j)!}\left[\frac{x_j}{\beta_j}\right]^l\frac{n_k!}{(n_k-m)!}Q^{(n_k-l\delta_{j,k})}_{(A-l\alpha_j)}(\mathbf{x}) .\end{aligned} \tag{39}$$

Here $(n_k-l\delta_{j,k})\ge 0$ and $(A-l\alpha_j)\ge 0$ with $m<n_k$ for Eq. (39). The sum of this equation over n_k results in Eq. (38) [cf. Eqs. (34) and (37)].

We now consider various average values in the canonical ensemble (Q_A) with the corresponding probability P_A:

$$P_A(\mathbf{n},\mathbf{x})=\frac{G_A(\mathbf{n},\mathbf{x})}{Q_A(\mathbf{x})}=\frac{A!\prod_{i=1}^{N}[x_i^{n_i}/(\beta_i^{n_i}n_i!)]}{\sum_{\{n_i\}_A}A!\prod_{i=1}^{N}[x_i^{n_i}/(\beta_i^{n_i}n_i!)]} . \tag{40}$$

The $P_A(\mathbf{n},\mathbf{x})$ is the probability for a specific partition $\mathbf{n}$ of A elements to appear. We also define $P_A(n_k,\mathbf{x})$ as the probability of having n_k species of type k,

$$P_A(n_k,\mathbf{x})=\sum_{\{n_i\}_{A,n_k}}P_A(\mathbf{n},\mathbf{x})=\frac{Q^{n_k}_A(\mathbf{x})}{Q_A(\mathbf{x})}=\frac{F^{n_k}_{A,m=0}(\mathbf{x})}{Q_A(\mathbf{x})} . \tag{41}$$

For these probabilities, using Eqs. (34) and (35), the average values of the factorial moments are

$$\begin{aligned}Y^m_A(k,\mathbf{x})=\left\langle\frac{n_k!}{(n_k-m)!}\right\rangle&=\sum_{n_k=0}^{\infty}\frac{n_k!}{(n_k-m)!}P_A(n_k,\mathbf{x})=\frac{\sum_{n_k=0}^{\infty}F^{n_k}_{A,m}(\mathbf{x})}{Q_A(\mathbf{x})}\\&=\frac{[x_k]^m[d/dx_k]^mQ_A(\mathbf{x})}{Q_A(\mathbf{x})}=\left[\frac{x_k}{\beta_k}\right]^m\frac{A!}{(A-m\alpha_k)!}\frac{Q_{(A-m\alpha_k)}(\mathbf{x})}{Q_A(\mathbf{x})} ,\end{aligned} \tag{42}$$

and the correlations between factorial moments are

$$\begin{aligned}&\langle n_k(n_k-1)\cdots(n_k-m+1)n_j(n_j-1)\cdots(n_j-l+1)\rangle\\&\quad=\sum_{\{n_i\}_A}\frac{n_j!}{(n_j-l)!}\frac{n_k!}{(n_k-m)!}P_A(\mathbf{n},\mathbf{x})=\frac{[x_j]^l[x_k]^m[d/dx_j]^l[d/dx_k]^mQ_A(\mathbf{x})}{Q_A(\mathbf{x})}\\&\quad=\left[\frac{x_j}{\beta_j}\right]^l\left[\frac{x_k}{\beta_k}\right]^m\frac{A!}{(A-m\alpha_k-l\alpha_j)!}\frac{Q_{(A-m\alpha_k-l\alpha_j)}(\mathbf{x})}{Q_A(\mathbf{x})}\\&\quad=Y^m_A(k,\mathbf{x})Y^l_{A-m\alpha_k}(j,\mathbf{x})=Y^m_{A-l\alpha_j}(k,\mathbf{x})Y^l_A(j,\mathbf{x}) .\end{aligned} \tag{43}$$

The $\langle\ \rangle$ represents an average over the canonical ensemble $Q_A(\mathbf{x})$. Equation (43) also applies for $j=k$ when $n_j=n_k-m$. For this case, Eq. (43) becomes Eq. (42) with the m of Eq. (42) set equal to $m+l$. The average of the factorial moments $Y^m_A(k,\mathbf{x})$ of Eq. (42) is zero for $m\alpha_k>A$, and the correlation between different factorial moments of Eq. (43) is zero unless $A-l\alpha_j-m\alpha_k\ge 0$.

The relations in Eqs. (42) and (43) give simple expressions for average moments and correlations of the cluster distribution n_k in the canonical ensemble. These quantities are expressed by a single ratio of canonical partition functions $Q_A(\mathbf{x})$ with different A values. As an illustration, the average number of species k in the canonical ensemble is, from Eq. (42),

$$\langle n_k \rangle = Y_A^1(k,\mathbf{x}) = \left[\frac{x_k}{\beta_k}\right] \frac{A!}{(A-\alpha_k)!} \frac{Q_{(A-\alpha_k)}(\mathbf{x})}{Q_A(\mathbf{x})} = \left[x_k \frac{d}{dx_k}\right] \ln Q_A(\mathbf{x}) \ . \tag{44}$$

The $\langle n_k \rangle$ is zero for the species k for which $\alpha_k > A$ in a nuclear fragmentation ($\alpha_i = i$). The corresponding correlations and fluctuations are, from Eq. (43),

$$\begin{aligned}\langle n_k n_j \rangle &= \left[\frac{x_j}{\beta_j}\right]\left[\frac{x_k}{\beta_k}\right] \frac{A!}{(A-\alpha_k-\alpha_j)!} \frac{Q_{(A-\alpha_k-\alpha_j)}(\mathbf{x})}{Q_A(\mathbf{x})} \\ &= Y_{(A-\alpha_j)}^1(k,\mathbf{x}) Y_A^1(j,\mathbf{x}) = Y_A^1(k,\mathbf{x}) Y_{(A-\alpha_k)}^1(j,\mathbf{x}) \ ,\end{aligned} \tag{45}$$

$$\begin{aligned}[\langle n_k^2 \rangle - \langle n_k \rangle^2] &= \left[x_k \frac{d}{dx_k}\right]^2 \ln Q_A(\mathbf{x}) \\ &= \left[\frac{x_k}{\beta_k}\right]^2 \frac{A!}{(A-2\alpha_k)!} \frac{Q_{(A-2\alpha_k)}(\mathbf{x})}{Q_A(\mathbf{x})} + \left[\frac{x_k}{\beta_k}\right] \frac{A!}{(A-\alpha_k)!} \frac{Q_{(A-\alpha_k)}(\mathbf{x})}{Q_A(\mathbf{x})} \\ &\quad - \left[\frac{x_k}{\beta_k}\right]^2 \left[\frac{A!}{(A-\alpha_k)!} \frac{Q_{(A-\alpha_k)}(\mathbf{x})}{Q_A(\mathbf{x})}\right]^2 \\ &= [Y_{(A-\alpha_k)}^1(k,\mathbf{x}) - Y_A^1(k,\mathbf{x}) + 1] Y_A^1(k,\mathbf{x}) \ .\end{aligned} \tag{46}$$

The left-hand side of Eq. (45) is to be taken as $\langle n_k(n_k-1) \rangle$ for the case of $j=k$. The correlations $\langle n_k n_j \rangle$ are zero for $(\alpha_k+\alpha_j) > A$ and the fluctuation in n_k is zero for $\alpha_k > A$. Notice here that the correlation $\langle n_k n_j \rangle$ is of a form very similar to the average distribution $Y_A^1(k,\mathbf{x}) = \langle n_k \rangle$. The averages and correlations for the cases $\alpha_i = \beta_i = 1$ and $\alpha_i = \beta_i = i$ are shown in Appendixes A and B, respectively. The detail behaviors of $\langle n_k \rangle$ and $\langle n_k n_j \rangle$ for the $\alpha_i = \beta_i = i$ case are studied in Ref. [2] for $x_i = xy^{\delta_{i,1}}$ and in Ref. [1] for $x_i = x$. Other choices of x_i's, which also are exactly soluble, are considered in Ref. [3] where applications to biological problems and social behavior are also discussed. The factorial moments [Eq. (42)] of the cluster distribution and their correlations [Eq. (43)] in our model are simple ratios of $Q_A(\mathbf{x})$ with different A values. This is a much simpler relation than the recursion relations of Ref. [7].

D. Microcanonical ensemble

In our approach exact microcanonical ensemble results can also be obtained since the relations of Eqs. (35)–(46) for Q_A are also true for Q_A^M of Eq. (22), which is the microcanonical ensemble partition function. For example, the average factorial moments of the cluster distribution in a microcanonical ensemble of fixed M and A becomes

$$\left\langle \frac{n_k!}{(n_k-m)!} \right\rangle_M = Y_A^m(k,\mathbf{x})_M = \left[\frac{x_k}{\beta_k}\right]^m \frac{A!}{(A-m\alpha_k)!} \frac{Q_{(A-m\alpha_k)}^{M-m}(\mathbf{x})}{Q_A^M(\mathbf{x})} \ . \tag{47}$$

Specifically, for $\alpha_i = \beta_i = i$ case with $x_i = x$ and $m=1$, Eq. (47) becomes, from Eq. (B2) in Appendix B,

$$\langle n_k \rangle_M = \left[\frac{1}{k}\right] \frac{A!}{(A-k)!} (-)^{k-1} \frac{S_{(A-k)}^{M-1}}{S_A^M} \ , \tag{48}$$

where S_A^M is the Stirling number of the first kind [1,4]. In this special case, $\langle n_k \rangle_M$ is independent of the parameter x. Similar results are easily found for the averages of all other factorial moments of the number distribution n_k for this microcanonical ensemble. The correlations between factorial moments in the microcanonical ensemble are

$$\begin{aligned}\left\langle \frac{n_k!}{(n_k-m)!} \frac{n_j!}{(n_j-l)!} \right\rangle_M &= \left[\frac{x_j}{\beta_j}\right]^l \left[\frac{x_k}{\beta_k}\right]^m \frac{A!}{(A-m\alpha_k-l\alpha_j)!} \frac{Q_{(A-m\alpha_k-l\alpha_j)}^{M-m-l}(\mathbf{x})}{Q_A^M(\mathbf{x})} \\ &= Y_A^m(k,\mathbf{x})_M Y_{A-m\alpha_k}^l(j,\mathbf{x})_{M-m} = Y_{A-l\alpha_j}^m(k,\mathbf{x})_{M-l} Y_A^l(j,\mathbf{x})_M \ .\end{aligned} \tag{49}$$

Due to Eq. (B2), these correlations are also independent of the parameter $x_i=x$ for the $\alpha_i=\beta_i=i$ case. Specifically,

$$\langle n_k n_j \rangle_M = \left[\frac{1}{j}\right]\left[\frac{1}{k}\right]\frac{A!}{(A-k-j)!}(-)^{k+j-2}\frac{S^{M-2}_{(A-k-j)}}{S^M_A} . \quad (50)$$

These behaviors are easy to understand since the generating function of $Q^M_A(\mathbf{x})$ defined by Eq. (22) is simply a multinomial of order M which is related to Eq. (14) without the summation over the multiplicity M. Hence, as can be seen in Eq. (4) for the $x_i=x$ case, all partitions have the same weighting factor x^M for fixed M.

Replacing the denominator Q^M_A which appears in Eqs. (47) and (49) by the canonical partition function Q_A gives the contribution of the partitions with multiplicity M to the average factorial moments and the correlations of the cluster distribution in the canonical ensemble. Explicitly,

$$\left[\frac{x_k}{\beta_k}\right]\frac{A!}{(A-\alpha_k)!}\frac{Q^{M-1}_{(A-\alpha_k)}(\mathbf{x})}{Q_A(\mathbf{x})}$$

represents the contribution of the partitions with multiplicity M to the average number of clusters $\langle n_k \rangle$ in the canonical ensemble. The total $\langle n_k \rangle$ in the canonical ensemble is then a sum over the contribution of different multiplicities M. The sum of $\langle n_k \rangle$ over k gives the average multiplicity M [cf. Eq. (3)]. Explicitly,

$$\langle M \rangle = \sum_{\{n_i\}_A}\left[\sum_{k=1}^{N} n_k\right]P_A(\mathbf{n},\mathbf{x}) = \sum_{k=1}^{N}\langle n_k \rangle . \quad (51)$$

In general, we define $P_A(M,\mathbf{x})$ as the probability of having M clusters regardless of the cluster sizes,

$$P_A(M,\mathbf{x}) = \sum_{\{n_i\}_{A,M}} P_A(\mathbf{n},\mathbf{x}) = \frac{Q^M_A(\mathbf{x})}{Q_A(\mathbf{x})} . \quad (52)$$

Then, moments of the multiplicity distribution are

$$\langle M^m \rangle = \sum_{M=0}^{\infty} M^m P_A(M,\mathbf{x}) = \sum_{M=0}^{\infty} M^m \frac{Q^M_A(\mathbf{x})}{Q_A(\mathbf{x})} . \quad (53)$$

We will come back to more detailed studies of the average multiplicity and its fluctuation in the following sections.

In this section, general expressions were developed for the grand canonical, canonical, and microcanonical partition functions for the clusterization of A constituent particles in Maxwell-Boltzmann statistics. These expressions can be used to study the cluster size distribution and the multiplicity distribution in the multifragmentation region of heavy-ion collision. Similar investigations with the counting rule of the Bose-Einstein or Fermi-Dirac type (Sec. II B) might be interesting problems. Especially, the Bose-Einstein-like distribution of Eq. (13), which does not have a microcounting factor such as $M_2(A,\mathbf{n})$ of Eq. (5), describes cracking of a nucleus through nucleon-nucleus collisions [5,6]. The number of partitions in this BE case is given by $p_{\rm BE}$ of Eq. (26). The Fermi-Dirac case [$p_{\rm FD}$ of Eq. (29)], which has limitation on the maximum number of clusters to be one, may be connected to sandpile problems [9]. Investigation of the relation between our model with the Fermi-Dirac statistics and the sandpile model of Ref. [9] is also an interesting problem which we hope to investigate in the future. The next section describes a general framework for studying the evolution of observables.

III. EVOLUTION OF OBSERVABLES

This section is concerned with an investigation of the underlying dynamical processes that produce the cluster size distribution function. We will also look at branching aspects of our dynamical model. These dynamical processes are studied by allowing the x_i's to change by letting them depend on a parameter. In the case of clusters, changes in the distribution of cluster sizes will be related to changes in the x_i's. The creation and disappearance of clusters through various underlying processes such as fission and fusion of clusters and by evaporation or pickup processes can be studied by this procedure of allowing the x_i's to vary in some parametric way. In the case of the branching aspects, the dynamical processes can be related to the evolution of a jet distribution.

Considering the weight parameter x_i's to be functions of an evolution parameter t such as time or temperature, i.e., $x_i=x_i(t)$, the changes induced by the variation of the parameter t can be studied. A change of the evolution parameter t of the system induces a change in the $x_i(t)$'s which assign a different weight given by $G_A(\mathbf{n},\mathbf{x})$ of Eq. (17) for different partitions $\mathbf{n}$. This change in the weight occurring in response to the change of the evolution parameter t of the system gives the t dependence of the partition function $Q_A(\mathbf{x})$ of Eq. (21) which describes the evolution of the system in t, i.e., how the distribution changes with t. We now develop expressions for changes in various distributions arising from changes in the $x_i(t)$'s coming from the parameter t.

For any function $\mathcal{F}(\mathbf{x})$ of x_i's,

$$\left[\frac{d}{dt}\right]\mathcal{F}(\mathbf{x}) = \sum_{k=1}^{N}\left[\frac{d}{dt}\ln x_k(t)\right]\left[x_k\frac{d}{dx_k}\right]\mathcal{F}(\mathbf{x}) , \quad (54)$$

$$\left[\frac{d}{dt}\right]^2\mathcal{F}(\mathbf{x}) = \sum_{j=1}^{N}\sum_{k=1}^{N}\left[\frac{d}{dt}\ln x_j(t)\right]\left[\frac{d}{dt}\ln x_k(t)\right]\left[x_j\frac{d}{dx_j}\right]\left[x_k\frac{d}{dx_k}\right]\mathcal{F}(\mathbf{x}) + \sum_{k=1}^{N}\left[\left[\frac{d}{dt}\right]^2\ln x_k(t)\right]\left[x_k\frac{d}{dx_k}\right]\mathcal{F}(\mathbf{x}) . \quad (55)$$

As an example, Eq. (32) gives, for G_A,

$$\left[\frac{d}{dt}\right] G_A(\mathbf{n},\mathbf{x}) = \sum_{k=1}^{N} \left[\frac{d}{dt}\ln x_k(t)\right] n_k G_A(\mathbf{n},\mathbf{x}) ,$$
$$\left[\frac{d}{dt}\right]^2 G_A(\mathbf{n},\mathbf{x}) = \sum_{k=1}^{N} \left[\left[\frac{d}{dt}\right]^2 \ln x_k(t)\right] n_k G_A(\mathbf{n},\mathbf{x}) + \sum_{j=1}^{N}\sum_{k=1}^{N} \left[\frac{d}{dt}\ln x_j(t)\right]\left[\frac{d}{dt}\ln x_k(t)\right] n_j n_k G_A(\mathbf{n},\mathbf{x}) . \tag{56}$$

Summing each equation of Eq. (56) over all the possible partitions of A gives the rates of change of the canonical partition function $Q_A(\mathbf{x})$ with parameter t which also determine the t dependences of observables, i.e., the mean cluster distribution $Y_A(k,\mathbf{x})$, mean multiplicity, fluctuations, correlations, etc.

When $x_i(t)=x_i t$, every species has the same t dependence independent of the species. From Eqs. (3), (21), (40), and (56), the following results can be obtained:

$$\left[t\frac{d}{dt}\right]\ln Q_A(t\mathbf{x})\Big|_{t=1} = \sum_{\{n_i\}_A} \left[\sum_{k=1}^{N} n_k\right] P_A(\mathbf{n},\mathbf{x}) = \langle M\rangle = \mathcal{M}_A(\mathbf{x}) , \tag{57}$$

and

$$\left[t\frac{d}{dt}\right]^2 \ln Q_A(t\mathbf{x})\Big|_{t=1} = \left[t\frac{d}{dt}\right]\mathcal{M}_A(t\mathbf{x})\Big|_{t=1} = \sum_{\{n_i\}_A} \left[\sum_{k=1}^{N} n_k\right]^2 P_A(\mathbf{n},\mathbf{x}) - \langle M\rangle^2$$
$$= [\langle M^2\rangle - \langle M\rangle^2] = \Delta\mathcal{M}_A(\mathbf{x}) . \tag{58}$$

Equation (57) is the average multiplicity $\mathcal{M}_A(\mathbf{x})$ [see Eq. (51)] in the canonical ensemble and Eq. (58) is its fluctuation $\Delta\mathcal{M}_A(\mathbf{x})$. For $\alpha_i=\beta_i=i$ and $x_i=xy^{\delta_{i,1}}$, the mean multiplicity and its fluctuation reduce to Eqs. (C1) and (C2) given in Appendix C, respectively. We can see from Eq. (58) that the evolution $(d\mathcal{M}_A/dt)$ of the mean multiplicity $\langle M\rangle$ is directly determined by its fluctuation $(\Delta\mathcal{M}_A)$ in this special case. This situation is easily understood. As can be seen in the weight Eq. (17), for the $x_i(t)=x_i t$ case, all the partitions with the same multiplicity M of Eq. (3) have the same t-dependent weight, t^M. This special case corresponds to the situation of a thermodynamic system made of species (clusters) having the same partition function independent of the detailed internal structure of the species (clusters) such as the free particle partition function arising from the thermal kinetic energy, $t\propto T^{3/2}$ [see $X_0(T)$ given by Eqs. (86) and (87) in Sec. IV].

If $x_i(t)=x_i t^{\alpha_i}$, as another special case, then Eq. (57) becomes the A of Eq. (16), which is the total number of elements for the $\alpha_i=i$ case, and Eq. (58) becomes zero which represents the conservation of the total number A. In this case, all the constituent particles have the same weight t, independent of the cluster (species) it belongs to. Thus all the partitions with fixed A have the same t-dependent weight, t^A. This situation corresponds to a thermodynamic partition function $t\propto e^{a_B/T}$ [cf., $X_1(T)$ of Eqs. (86) and (87)] arising from the binding energy per particle a_B in a cluster which is assumed to be independent of the cluster size.

A. Evolution of the distribution $F_{A,m}^{n_k}(\mathbf{x})$ of species k and branching processes: Furry distribution

This subsection will investigate the evolution of the quantity $F_{A,m}^{n_k}(\mathbf{x})$ given by Eq. (34). At $m=0$, the $F_{A,0}^{n_k}(\mathbf{x})/Q_A(\mathbf{x})=Q_A^{n_k}(\mathbf{x})/Q_A(\mathbf{x})$ is the probability of having n_k species of type k as already noted in Eq. (41). Also $F_{A,m}^{n_k}(\mathbf{x})/Q_A(\mathbf{x})$ summed over n_k gives the ensemble averaged quantity $Y_A^m(k,\mathbf{x})=\langle n_k(n_k-1)\cdots(n_k-m+1)\rangle$ which is discussed in Sec. III B. The evolution of the $F_{A,m}^{n_k}(\mathbf{x})$ contains information regarding the underlying dynamics such as in various cascade phenomena. From Eq. (54), we obtain the dynamic equation for the function $F_{A,m}^{n_k}(\mathbf{x})$ of Eq. (34);

$$\left[\frac{d}{dt}\right] F_{A,m}^{n_k}(\mathbf{x}) = \frac{A}{\alpha_k}\left[\frac{d}{dt}\ln x_k(t)\right] F_{A,m}^{n_k}(\mathbf{x}) + \sum_{j=1}^{N} \left[\frac{d}{dt}\ln x_j(t) - \left[\frac{\alpha_j}{\alpha_k}\right]\frac{d}{dt}\ln x_k(t)\right]\left[\frac{x_j}{\beta_j}\right]\frac{A!}{(A-\alpha_j)!} F_{(A-\alpha_j),m}^{n_k}(\mathbf{x}) . \tag{59}$$

See Eq. (D1) in Appendix D for more detailed steps regarding Eq. (59).

An interesting application of Eq. (59) is to branching processes and jet fragmentation. For $\alpha_i=\beta_i=1$, Eq. (59) reduces to

$$\frac{d}{dt} F_{A,m}^{n_k}(\mathbf{x}) = A\left[\frac{d}{dt}\ln x_k\right] F_{A,m}^{n_k}(\mathbf{x}) + A\sum_{j=1}^{N}\left[\frac{d}{dt}\ln\left[\frac{x_j}{x_k}\right]\right] x_j F_{(A-1),m}^{n_k}(\mathbf{x}) . \tag{60}$$

Furthermore, if $N=2$ with $x_1(t)=1/\omega(t)$ and $x_2(t)=1-1/\omega(t)$, then

$$\frac{d}{dt}\tilde{F}^{n_k}_{A,m}(\mathbf{x})=-\left[\frac{1}{\omega}\frac{d\omega}{dt}\right][A\tilde{F}^{n_k}_{A,m}(\mathbf{x})-(A-m)\tilde{F}^{n_k}_{(A-1),m}(\mathbf{x})] \tag{61}$$

for $k=1$, where $\tilde{F}$ is defined by the relation

$$F^{n_k}_{A,m}(\mathbf{x})=\frac{A!}{(A-m\alpha_k)!}\tilde{F}^{n_k}_{A,m}(\mathbf{x}) . \tag{62}$$

Equation (61) is a generalization of a dynamical equation ($m=1$) for the multiplicity distribution function of jet fragmentation in ϕ^3 theory [8] having three lines at each vertex. Then the solution of Eq. (61) becomes the Furry distribution

$$\tilde{F}^{n_k}_{A,1}=\frac{\Gamma(A)}{\Gamma(n_k)\Gamma(A-n_k+1)}\left[\frac{1}{\omega}\right]^{n_k}\left[1-\frac{1}{\omega}\right]^{A-n_k}$$

in ϕ^3 theory with the evolution parameter $\omega(t)=e^{\beta t}$. Here the A is the number of final jet lines at t and n_k is the number of initial jet lines at $t=0$. In ϕ^3 theory, each initial line (stem) branches into $N=2$ new lines (branches) at each step. Detailed discussions concerning the relation between Furry distribution and branching processes can be found in Ref. [8].

For the situation of $\alpha_i=\beta_i=i$ with $x_i(t)=x(t)$, we get, from Eq. (59),

$$\frac{d}{dt}F^{n_k}_{A,m}(\{x_i=x\})=\left[\frac{d}{dt}\ln x\right]\left[\frac{A}{k}F^{n_k}_{A,m}(\{x_i=x\})+\sum_{j=1}^{N}\left[\frac{x}{j}\right]\frac{(k-j)}{k}\frac{A!}{(A-j)!}F^{n_k}_{(A-j),m}(\{x_i=x\})\right] \tag{63}$$

or

$$\frac{d}{dt}\tilde{F}^{n_k}_{A,m}(\{x_i=x\})=\left[\frac{d}{dt}\ln x\right]\left[\frac{A}{k}\tilde{F}^{n_k}_{A,m}(\{x_i=x\})+\sum_{j=1}^{N}\left[\frac{x}{j}\right]\frac{(k-j)}{k}\frac{(A-mk)!}{(A-mk-j)!}\tilde{F}^{n_k}_{(A-j),m}(\{x_i=x\})\right] .$$

These results may be considered dynamical equations for the factorial distribution of clusters of size k in a nuclear fragmentation. The first term in either equation represents the dependence on the multiplicity n_k of the same species k and the second term represents the dependence on the multiplicity n_j of clusters of size $j\neq k$. Equation (63) for $m=1$ is the changing rate of the number of clusters of size k, n_k, when each cluster has the same weight $x(t)$ independent of the size, an example is the partition function $x(t)\propto T^{3/2}$ arising from the thermal kinetic energy of the cluster.

B. Evolution of mean distribution and equilibrium: Fokker-Planck equation

The evolution of the average number of clusters of size k can also be obtained. We will also show how the results developed in this section can be reduced to a Fokker-Planck equation. The evolution of the average factorial moments is given by [from Eq. (D2) in Appendix D]

$$\begin{aligned}\frac{d}{dt}Y^m_A(k,\mathbf{x})&=\sum_{j=1}^{N}\left[\frac{d}{dt}\ln x_j(t)\right]\left[\left\langle n_j\frac{n_k!}{(n_k-m)!}\right\rangle-\langle n_j\rangle\left\langle\frac{n_k!}{(n_k-m)!}\right\rangle\right]\\&=\sum_{j=1}^{N}\left[\left[\frac{d}{dt}\right]\ln x_j(t)-\left[\frac{\alpha_j}{\alpha_k}\right]\left[\frac{d}{dt}\right]\ln x_k(t)\right]Y^1_A(j,\mathbf{x})[Y^m_{(A-\alpha_j)}(k,\mathbf{x})-Y^m_A(k,\mathbf{x})] .\end{aligned} \tag{64}$$

Notice here that, from Eq. (42),

$$Y^m_{(A-l\alpha_j)}(k,\mathbf{x})Y^l_A(j,\mathbf{x})=Y^m_A(k,\mathbf{x})Y^l_{(A-m\alpha_k)}(j,\mathbf{x}) . \tag{65}$$

When $m=1$, $Y^1_A(k,\mathbf{x})$ is the mean number of cluster $\langle n_k\rangle$ and Eq. (64) reduces to

$$\begin{aligned}\frac{d}{dt}Y^1_A(k,\mathbf{x})=\frac{d}{dt}\langle n_k\rangle&=\sum_{j=1}^{N}\left[\frac{d}{dt}\ln x_j(t)\right][\langle n_jn_k\rangle-\langle n_j\rangle\langle n_k\rangle]\\&=\sum_{j=1}^{N}\left[\left[\frac{d}{dt}\right]\ln x_j(t)-\left[\frac{\alpha_j}{\alpha_k}\right]\left[\frac{d}{dt}\right]\ln x_k(t)\right]Y^1_A(j,\mathbf{x})[Y^1_{(A-\alpha_j)}(k,\mathbf{x})-Y^1_A(k,\mathbf{x})] .\end{aligned} \tag{66}$$

This result shows that the change of the average multiplicity $(d\langle n_k\rangle/dt)$ of species k is directly related to the fluctuation $(\langle n_k^2\rangle-\langle n_k\rangle^2)$ and the correlations $(\langle n_jn_k\rangle-\langle n_j\rangle\langle n_k\rangle)$. Thus, to study dynamical properties associated with fragmentation phenomena in heavy-ion collisions, the fluctuations and correlations, besides the average multiplicity, must be considered. Equation (66) shows that a system is in an equilibrium state, if all the fluctuations and the correlations are zero, i.e., $\langle n_j n_k \rangle = \langle n_j \rangle \langle n_k \rangle$, but not vice versa in general.

Separating $j<k$ and $j>k$ and defining N_k^m as

$$N_k^m(A) = \alpha_k Y_A^m(k,\mathbf{x}) \ , \tag{67}$$

Eq. (64) can be rewritten as

$$\begin{aligned} \frac{d}{dt} N_k^m(A) = & \sum_{l=1}^{k-1} C_{(k-l)}^l N_k^m(A-\alpha_{(k-l)}) N_{(k-l)}^1(A) - \sum_{l=1}^{N-k} C_k^l N_k^m(A-\alpha_{(k+l)}) N_{(k+l)}^1(A) \\ & - \sum_{l=1}^{k-1} C_{(k-l)}^l N_k^m(A) N_{(k-l)}^1(A) + \sum_{l=1}^{N-k} C_k^l N_k^m(A) N_{(k+l)}^1(A) \ , \end{aligned} \tag{68}$$

where

$$C_k^l = \left[\frac{1}{\alpha_k} \left[\frac{d}{dt} \right] \ln x_k(t) - \frac{1}{\alpha_{(k+l)}} \left[\frac{d}{dt} \right] \ln x_{(k+l)}(t) \right] = -C_{k+l}^{-l} \ . \tag{69}$$

The first two terms in Eq. (68) can be rewritten using the relation

$$N_k^m(A-\alpha_j) N_j^1(A) = N_k^m(A) N_j^1(A - m\alpha_k) \tag{70}$$

due to Eq. (65). For the case of $\alpha_i = i$, $N_k^1(A) = k\langle n_k \rangle$ can be considered as the total average number of nucleons belonging to clusters of size k in the fragmentation of a nucleus of size A. The quantity $N_k^1(A)/A = (k/A)\langle n_k \rangle$ is considered in Ref. [3] as a probability. While Eq. (68) seems complex, this equation has a simple interpretation. The first term of Eq. (68) represents the creation of species k arising from the fusion of one of the $N_{(k-l)}^1(A)$ species $(k-l)$ and one of species l [process (a) in Fig. 1] when the $C_{(k-l)}^l$ is positive. If the $C_{(k-l)}^l$ is negative, we can also interpret this same term as an annihilation process (b) of one of $N_k^1(A)$ species k using the right-hand side representation of Eq. (70) which has $N_k^m(A)$. The second term of Eq. (68) represents the formation of species $(k+l)$ arising from the fusion of species k and l [process (c) in Fig. 1], which thus reduces species k, using the right-hand side representation of Eq. (70) when C_k^l is positive. When C_k^l is negative, this second term represents the formation of species k arising from the fission of species $(k+l)$ [process (d) in Fig. 1] using the left-hand side representation of Eq. (70). The third term represents the annihilation of species k due to its fragmentation into species $(k-l)$ and l [process (b) in Fig. 1] for $C_{(k-l)}^l > 0$, or the creation of species k through the fusion of species $(k-l)$ and l [process (a) in Fig. 1] for $C_{(k-l)}^l < 0$. Finally, the fourth term represents the increase of species k due to the fission of the species $(k+l)$ into k and l [process (d) in Fig. 1] when C_k^l is positive, or the decrease of species k through the fusion with the species l [process (c) in Fig. 1] when C_k^l is negative.

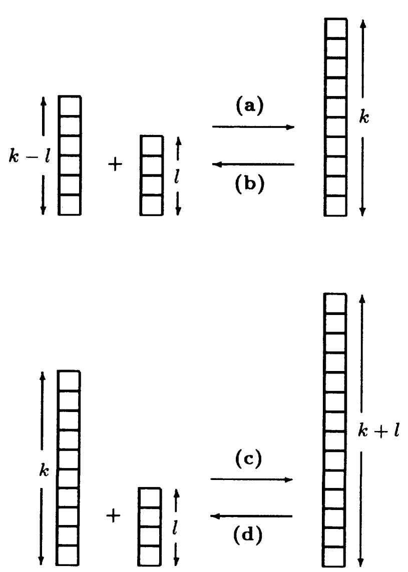

FIG. 1. Evolution of fragmentation process in the fragmentation block diagram representation [3]. Each box represents a nucleon and the stack of boxes represents a cluster.

An expression for how the mth factorial moment of the distribution of species k evolves with t can be obtained using Eq. (68). It is easy to see that the distribution is stable, i.e., $(d/dt)N_k^m(A)=0$, if $x_i(t) = x_i[f(t)]^{\alpha_i}$ since $C_k^l = 0$ due to Eq. (69) for this case. Defining a current as

$$\begin{aligned} J_j^l(A,k,m) &= C_j^l N_k^m(A-\alpha_j) N_j^1(A) - C_j^l N_k^m(A) N_j^1(A) \\ &= C_j^l N_k^m(A) N_j^1(A - m\alpha_k) \\ &\quad - C_j^l N_k^m(A) N_j^1(A) \ , \end{aligned} \tag{71}$$

Eq. (68) can be rewritten as

$$\frac{d}{dt} N_k^m(A) = \sum_{l=1}^{k-1} J_{(k-l)}^l(A,k,m) + \sum_{l=1}^{N-k} J_{(k+l)}^{-l}(A,k,m) \ . \tag{72}$$

The evolution of the average distribution $\langle n_k \rangle$ corresponds to the $m=1$ case. The distribution is in equilibrium when $J_j^l(A,k,m)=0$.

For $\alpha_i = \beta_i = i$ and $x_i(t) = x(t)$, using Eq. (B4) in Appendix B with $y=1$,

$$J_j^l(A,k,m)=l\left[\frac{d}{dt}\ln x(t)\right]\left[\frac{x}{j}\right]\frac{A!}{(A-j)!}\frac{\Gamma(x+A-j)}{\Gamma(x+A)}\left[\frac{x}{k}\right]^m \times\left[\frac{(A-j)!}{(A-mk-j)!}\frac{\Gamma(x+A-mk-j)}{\Gamma(x+A-j)}\theta(A-mk-j)-\frac{A!}{(A-mk)!}\frac{\Gamma(x+A-mk)}{\Gamma(x+A)}\theta(A-mk)\right] . \tag{73}$$

The step function $\theta(a)$ is 1 for $a\geq 0$ and is zero otherwise. When $x=0$ or $x=\infty$, $J_j^l(A,k,m)=0$ for all l, $-(N-k)\leq l\leq(k-1)$, independently of A and k, i.e., the distribution is in equilibrium. For $mk+j\leq A$, $J_j^l(A,k,m)=0$ at $x=1$. Thus at $x=1$, the distribution can be changed only through the growth or loss process arising from clusters of size j with $A-mk<j\leq A$.

On the other hand, for $\alpha_i=\beta_i=1$, using Eq. (A2) in Appendix A,

$$J_j^l(A,k,m)=-m\frac{A!}{(A-m)!}\left[\frac{d}{dt}\ln\frac{x_j(t)}{x_k(t)}\right]\left[\frac{x_j}{\sum_i x_i}\right]\left[\left[\frac{x_k}{\sum_i x_i}\right]^m\right] . \tag{74}$$

The current of Eq. (74) is zero only when $x_k=0$ or $x_j=0$ or $(d/dt)\ln[x_j(t)/x_k(t)]=0$, i.e., x_j and x_k have the same t dependence. Otherwise, this current is nonzero and describes the branching process studied in Ref. [8].

For the $m=1$ case, Eq. (68) or (72) represents the evolution of the average distribution of species k,

$$\frac{d}{dt}N_k^1(A)=\sum_{l=1}^{k-1}D_{(k-l)}^lN_{(k-l)}^1(A)-\left[\sum_{l=1}^{N-k}D_k^l+\sum_{l=1}^{k-1}E_k^l\right]N_k^1(A)+\sum_{l=1}^{N-k}E_{(k+l)}^lN_{(k+l)}^1(A) , \tag{75}$$

where

$$D_j^l=C_j^lN_{(j+l)}^1(A-\alpha_j) ,$$
$$E_j^l=C_{(j-l)}^lN_{(j-l)}^1(A) . \tag{76}$$

The result of Eq. (75) can be related to a Fokker-Planck equation [8,10] by considering only $l=1$ and going to the continuum limit of k. That is, using

$$E_{(k+1)}^1N_{(k+1)}^1(A)\approx E_k^1N_k^1(A)+\frac{\partial}{\partial k}E_k^1N_k^1(A)+\frac{1}{2!}\frac{\partial^2}{\partial k^2}E_k^1N_k^1(A) ,$$

and with a similar approximation for $D_{(k-1)}^1N_{(k-1)}^1(A)$, Eq. (75) is reduced to

$$\frac{d}{dt}N_k^1(A)=\frac{\partial}{\partial k}\left[(E_k^1-D_k^1)N_k^1(A)+\frac{1}{2}\frac{\partial}{\partial k}(E_k^1+D_k^1)N_k^1(A)\right] . \tag{77}$$

A continuum k limit of Eq. (75) becomes the differential form of the Chapman-Kolmogorov equation [8]. Due to the discrete value of k, Eq. (75) is applicable to a finite system with the finite number of k values.

IV. EXPECTATION VALUES AND VARIOUS SPECIAL TEMPERATURES

This section considers the thermodynamic properties in a nuclear fragmentation; how nucleons in a nuclear system at moderate energy are redistributed among clusters, and how the initial energy affects the modes of fragmentation of the nucleus. The previous section considered the evolution of the distribution using an evolution parameter t for the weight parameter $x_i(t)$'s by looking at the change of the system in response to the change of t. Here we will relate the parameter t to the inverse temperature $t=1/T$ and the weight parameter $x_i(t)$ of cluster i to the thermodynamic partition function of the cluster at a given temperature $T=1/t$. By looking at the cluster distribution at a fixed temperature T, we can study the thermodynamic properties of a system with given excitation energy in a fragmentation process. Different excitation energy or temperature gives different weight $x_i(T)$ for clusters which induce different cluster distribution in the system.

Consider some quantity $f_i(t)$ which characterizes the species i such as the energy of a cluster of size i in the fragmentation of a nucleus. To find the average value of the total quantity $f(t)$ defined by

$$f(t)=\sum_{i=1}^{N}f_i(t)n_i , \tag{78}$$

let the t dependence of $x_i(t)$ be

$$x_i(t)=\tilde{x}_i\exp\left[\int^t f_i(t)dt\right] . \tag{79}$$

Then from Eq. (56), the expectation value of $f(t)$ with the probability $P_A(\mathbf{n},\mathbf{x})$ defined in Eq. (40) is

$$\langle f(t)\rangle=\sum_{\{n_i\}_A}\sum_{k=1}^{N} f_k(t)n_kP_A(\mathbf{n},\mathbf{x})=\sum_{k=1}^{N} f_k(t)\langle n_k\rangle=\left[\frac{d}{dt}\right]\ln Q_A(\mathbf{x}) . \tag{80}$$

The last equality follows from Eq. (44). Also, the change of the expectation value in t is

$$\begin{aligned}\frac{d}{dt}\langle f(t)\rangle&=\left[\frac{d}{dt}\right]^2\ln Q_A(\mathbf{x})\\&=\sum_{k=1}^{N}\sum_{j=1}^{N} f_j(t)f_k(t)[\langle n_jn_k\rangle-\langle n_j\rangle\langle n_k\rangle]+\sum_{k=1}^{N}\left[\frac{d}{dt}f_k(t)\right]\langle n_k\rangle\\&=\langle[f(t)]^2\rangle-[\langle f(t)\rangle]^2+\left\langle\left[\frac{d}{dt}f(t)\right]\right\rangle .\end{aligned}\tag{81}$$

Notice here that n_k is independent of t even though $\langle n_k\rangle=Y_A^1(k,\mathbf{x})$ depends on t through $x_i(t)$. Thus $f(t)$ of Eq. (78) has a t dependence only through the explicit t dependence of $f_i(t)$. However $\langle f(t)\rangle$ has a t dependence through both of $f_k(t)$ and $\langle n_k\rangle=Y_A^1(k,\mathbf{x}(t))$. Equation (81) shows that the rate of change of $\langle f(t)\rangle$ with respect to t is the same as the fluctuation of $f(t)$, i.e., $\langle f^2(t)\rangle-\langle f(t)\rangle^2$ if $f_k(t)$ is t independent. As a special case, evaluating Eqs. (80) and (81) at $t=0$ with $f_k(t)=1$ [which corresponds to $f(t)=\sum_{k=1}^{N}n_k=M$] generates the average multiplicity and its fluctuation which are given by Eqs. (57) and (58). On the other hand, if we put $f_k(t)=\alpha_k$, then $f(t)=\sum_{k=1}^{N}\alpha_kn_k=A$.

A. Parameter x_i as a thermodynamic variable

To study cluster size distributions in nuclear fragmentations, we identify a cluster i by the number of nucleons in the cluster; then $\alpha_i=i$. Moreover, we will consider only the special case $\alpha_i=\beta_i=i$ [Eq. (B1) in Appendix B] with $N=\infty$ (actually $N=A$ for the case with fixed A, i.e., $n_i=0$ for $i>A$). Here the choice $\beta_i=i$ accounts for the cyclic rearrangement of nucleons in each of n_i clusters.

Relating $f_i(t)$ with the energy E_i of a cluster i and the parameter t with the inverse temperature T, our formulations can be used to study a fragmentation of a nucleus at finite temperature T. Through this connection, the weight parameter x_i of Eq. (79) becomes the usual partition function of the cluster in thermodynamics. Neglecting the surface energy and the Coulomb energy, the energy E_i of a cluster with i nucleons is of the form

$$E_i(T)=\mathcal{E}_0(T)+\mathcal{E}_1(T)i+\mathcal{E}_y(T)\delta_{i,1} . \tag{82}$$

The $\mathcal{E}_0$ is independent of the size of a cluster such as its mean kinetic energy at a given temperature T and the second term depends on the size such as the binding energy in the cluster. The $\mathcal{E}_y$ term is introduced because that monomer has no binding or internal excitation energy. For a cluster of size i with the energy given by [11,12]

$$E_i(T)=\frac{3}{2}T+M_Bi-\left[a_B-\frac{1}{\epsilon_0}\left[\frac{T_0T}{T+T_0}\right]^2\right]i ,$$

these terms are

$$\begin{aligned}\mathcal{E}_0(T)&=\frac{3}{2}T ,\\\mathcal{E}_1(T)&=M_B-a_B+\frac{1}{\epsilon_0}\left[\frac{T_0T}{T+T_0}\right]^2 ,\\\mathcal{E}_y(T)&=a_B-\frac{1}{\epsilon_0}\left[\frac{T_0T}{T+T_0}\right]^2 .\end{aligned}\tag{83}$$

In Eq. (83), the Boltzmann constant $k_B=1$, M_B is the nucleon mass, a_B is the binding energy per nucleon in a nucleus, ϵ_0 is the nuclear level density parameter for internal excitations, and T_0 is the cutoff temperature for the excitation level density. Experimentally, $a_B\approx 8$ MeV and $\epsilon_0\approx 8$ MeV for a finite nucleus [11] and these values are about half of the values in nuclear matter.

Identifying the quantity $-f_i(t)$ as the energy $E_i(T)$ of a cluster with i nucleons at temperature $T=1/t$,

$$f_i(t=1/T)=-E_i(T)=-\mathcal{E}_0(T)-\mathcal{E}_1(T)i-\mathcal{E}_y(T)\delta_{i,1} , \tag{84}$$

the total energy of the system is then

$$\begin{aligned}E(T)&=-f(t=1/T)=-\sum_i f_i(t)n_i\\&=\mathcal{E}_0(T)M+\mathcal{E}_1(T)A+\mathcal{E}_y(T)n_1 .\end{aligned}\tag{85}$$

Here the nucleon number A and the multiplicity M are given by Eqs. (2) and (3), respectively. Then the weight variable $x_i(t)$ of Eq. (79) is

$$x_i(t=1/T)=X_0(T)X_1^i(T)y^{\delta_{i,1}}(T) , \tag{86}$$

with

$$X_0(T=1/t)=x(v)\exp\left[-\int^t \mathcal{E}_0(T)dt\right]$$
$$=x(v)T^{3/2} ,$$

$$X_1(T=1/t)=\exp\left[-\int^t \mathcal{E}_1(T)dt\right]$$
$$=\exp\left[-\frac{(M_B-a_B)}{T}+\frac{1}{\epsilon_0}\left[\frac{T_0T}{T+T_0}\right]\right] , \quad (87)$$

$$y(T=1/t)=\exp\left[-\int^t \mathcal{E}_y(T)dt\right]$$
$$=\exp\left[-\frac{a_B}{T}-\frac{1}{\epsilon_0}\left[\frac{T_0T}{T+T_0}\right]\right] .$$

The last relation of Eq. (87) shows that $y \le 1$ and $y=1$ at $T=\infty$ and $T_0=0$ (T, a_B, ϵ_0 are all positive). This result also shows that there is no monomer at zero temperature since $y=0$ at $T=0$ [cf. x-y model of Eq. (B4) in Appendix B]. At high temperature, the cluster distribution depends on the value of the cutoff temperature T_0. The situation $T_0=0$ or equivalently $\epsilon_0=\infty$ corresponds to having no bound excited levels in a cluster ($y=1$ at $T=\infty$ for this choice of cutoff temperature T_0). At the other extreme, the choice of $T_0=\infty$ corresponds to having bound levels with infinite excitation energy. Moreover, when $T=\infty$, $y=0$ and thus x_1 is zero and no monomers are present which is unphysical. Thus we should use a finite cutoff temperature T_0. $X_0(T)$, $X_1(T)$, and $y(T)$ are all zero at $T=0$. At high temperature T, as $T\to\infty$, $X_1(T)=\exp(T_0/\epsilon_0)$, and $y(T)=\exp(-T_0/\epsilon_0)$ are finite while $X_0(T)\to\infty$ (see Appendix F). The partition functions and the mean cluster distributions for $x_i=X_0X_1^iy^{\delta_{i,1}}$ of Eq. (86) are given in Appendix E.

The $x_i(t)$ of Eq. (79) corresponds to the partition function $z_i(T)=e^{-F_i(T)/T}$ of cluster i. Here the free energy $F_i(T)$ is given by

$$F_i(T)=T\int^t E_i(T)dt=-T\int^T \frac{E_i(T)}{T^2}dT . \quad (88)$$

The integral over t here and in Eq. (87) or (79) is the generalization to a T-dependent Hamiltonian E_i of a cluster i. This integral is similar to the action in a path integral with a time dependent Hamiltonian. For a system with the energy given by Eq. (85) or equivalently by (82), the partition function x_i of a cluster has three pieces shown in Eqs. (86) and (87); (i) a cluster size independent part $X_0(T)$ which originates from the thermal kinetic energy of a cluster together with the volume dependence of the system, (ii) $X_1(T)$ which is the same for every nucleon independent of the cluster it belongs to and arises from the binding energy per nucleon in a cluster and the mass energy, (iii) $y(T)$ which distinguishes monomers, i.e., free nucleons, from clusters due to the lack of binding energy or internal structure of the monomers.

B. Thermodynamic quantities: energy, entropy, and pressure

Using expressions just developed, in particular Eqs. (84)–(87), the ensemble averaged behavior of thermodynamical quantities can be developed. As an example, we can find the average energy of the system at a given T and its change with T in a canonical ensemble (fixed A). Using these equations and Eq. (80), we find, for the mean energy of a system with the cluster energy E_i given by Eq. (82),

$$\langle E(T)\rangle=-\langle f(t=1/T)\rangle=-\left[\frac{d}{dt}\right]\ln Q_A(\mathbf{x})$$
$$=\mathcal{E}_0(T)\langle M\rangle+\mathcal{E}_1(T)A+\mathcal{E}_y(T)\langle n_1\rangle . \quad (89)$$

For the change in energy with T, we obtain the result, from Eq. (81),

$$T^2\left[\frac{d}{dT}\right]\langle E(T)\rangle=-\left[\frac{d}{dt}\right]\langle E(T)\rangle$$
$$=\mathcal{E}_0^2(T)[\langle M^2\rangle-\langle M\rangle^2]+\mathcal{E}_y^2(T)[\langle n_1^2\rangle-\langle n_1\rangle^2]-\frac{d\mathcal{E}_0(T)}{dt}\langle M\rangle-\frac{d\mathcal{E}_1(T)}{dt}A-\frac{d\mathcal{E}_y(T)}{dt}\langle n_1\rangle , \quad (90)$$

where

$$\frac{d\mathcal{E}_0(T)}{dt}=-\frac{3}{2}T^2 ,$$
$$\frac{d\mathcal{E}_1(T)}{dt}=-\frac{2}{\epsilon_0}\left[\frac{T_0T}{T+T_0}\right]^3 , \quad (91)$$
$$\frac{d\mathcal{E}_y}{dt}=\frac{2}{\epsilon_0}\left[\frac{T_0T}{T+T_0}\right]^3 .$$

The average multiplicity $\langle M\rangle$ and its fluctuation $[\langle M^2\rangle-\langle M\rangle^2]$ are given by Eqs. (C1) and (C2) with $x=X_0(T)$. From Eq. (90), we can find the heat capacity $C_V=d\langle E\rangle/dT$. The last three terms in Eq. (90) are the average of $dE(T)/dt=-df(t)/dt$ [see Eq. (81)] and the first two terms are the fluctuation of the total energy,

$$\langle E^2(T)\rangle-\langle E(T)\rangle^2=\mathcal{E}_0^2(T)[\langle M^2\rangle-\langle M\rangle^2]$$
$$+\mathcal{E}_y^2(T)[\langle n_1^2\rangle-\langle n_1\rangle^2] . \quad (92)$$

This fluctuation is always non-negative as well as the fluctuation of multiplicity. Due to the asymptotic behavior of Eqs. (F6) and (F8) for the $x_i(t)$ of Eq. (86), the fluctuation of the energy Eq. (92) is zero at both of $T=0$ and $T=\infty$. Since $\Delta\mathcal{M}_A(X_0,y)\propto X_0=x(v)T^{3/2}$ and $[\langle n_1^2\rangle-\langle n_1\rangle^2]\propto y\approx e^{-a_B/T}$ at low T (see Appendix F), the energy fluctuation goes to zero with $T^{7/2}$ as $T\rightarrow 0$. Furthermore, $\langle M\rangle\approx 1$ and $\langle n_1\rangle\propto y\approx e^{-a_B/T}$ at low temperature and $\langle M\rangle\approx A$ and $\langle n_1\rangle\approx A$ as $T\rightarrow\infty$. Thus, from Eq. (90), at $T=0$ and ∞, $C_V=d\langle E(T)\rangle/dT=\frac{3}{2}\langle M\rangle$. This behavior in C_V for a system with Eq. (85) has its origin in the kinetic energy of clusters at T; $d\mathcal{E}_0(T)/dT=\frac{3}{2}$ for each cluster independent of its size.

The canonical partition function Q_A determines the free energy $F=-T\ln Q_A$. The corresponding entropy $S=-\partial F/\partial T$ can then be evaluated by

$$S=t(\langle E\rangle-F)=t\langle E\rangle+\ln Q_A(\mathbf{x}) , \qquad (93)$$

where the average energy $\langle E\rangle$ is given by Eq. (89) and Q_A is given by Eq. (E1). Using the grand canonical partition function Q given by Eq. (E1), we can find the pressure of the system as

$$P(T)=\frac{T}{V(T)}\ln Q(u,\mathbf{x}) . \qquad (94)$$

To determine $P(T)$, we need to know the volume V of the system. The quantity $x(v)$ in $X_0=x(v)T^{3/2}$ of Eq. (87) represents the volume dependence of x_i. To approximate this volume dependence of $x(v)$, we consider the partition function of free particles gV_f/λ_i^3, where g is the degeneracy, $V_f=V-V_0$ is the free volume available to the cluster with i nucleons, and $\lambda_i=\sqrt{2\pi\hbar^2/m_iT}$ is the thermal wavelength of the cluster with mass m_i. Then in terms of the average volume v per nucleon and mass M_B of a nucleon, the free particle partition function of the cluster becomes

$$\frac{gV_f}{\lambda_i^3}=\frac{g}{h^3}A(v-v_0)(2\pi M_B)^{3/2}i^{3/2}T^{3/2} . \qquad (95)$$

Here A is the total number of participant nucleons in the system and $\rho_0=1/v_0$ is the nuclear matter saturation density. If we neglect the size i dependence in Eq. (95), we can consider this partition function of Eq. (95) as the $X_0=x(v)T^{3/2}$ in Eq. (87). Then, we have

$$x(v)=\frac{g}{h^3}(2\pi M_B)^{3/2}A(v-v_0)$$
$$=\frac{g(2\pi M_B)^{3/2}}{h^3\rho_0}A\left[\left[\frac{\rho_0}{\rho}\right]-1\right] , \qquad (96)$$

where ρ is the average nuclear density. The ratio ρ_0/ρ represents the expansion of the system compared to nuclear matter with the saturation density ρ_0.

C. Various temperatures in nuclear fragmentation

For a nuclear system which has about 50 or more nucleons, we can easily evaluate Eqs. (E1)–(E4) only for small values of X_0 and y, i.e., only for low temperature [see Eq. (87)]. However if $y=1$, Q_A of Eq. (E1) becomes very simple (only one term with $r=A$ survives) and there is no problem evaluating the multiplicity and other quantities even at very high temperatures with large X_0. Thus, as in Ref. [1], we will first consider the case $y=1$ which is obtained by replacing $X_0y^{\delta_{i,1}}$ in Eq. (86) with X_0y. This case corresponds to using the backshifted binding energy $E_B(i)=a_B(i-1)$ instead of $E_B(i)=a_Bi$ used in Eq. (83).

Table I and Fig. 2 show the T dependence of $\langle E\rangle$, $\langle M\rangle$, $\langle n_1\rangle$, and their fluctuations for $0<T<\infty$. Figure 2 also shows the evolution of observables ($\langle E\rangle$, $\langle M\rangle$, and $\langle n_1\rangle$) in response to the change of the temperature T. Higher T corresponds to larger X_0 and thus system fragments into more pieces. Here, $A(\rho_0/\rho-1)=200$ is used for $x(v)$ of Eq. (96) which gives $x(v)=1.31$ with a fixed total volume V. The corresponding value of ρ_0/ρ is 3 for $A=100$, which is the value used in Ref. [12] for $A=100$ nucleons, and $\rho_0/\rho=5$ for $A=50$, which is similar to the lower density of the spinodal point at $T=15.77$ MeV discussed later.

Here we can consider various temperatures related to several different kinds of phenomena in the nuclear fragmentation process [13]. The results of our calculations show that the system starts to fragment (average multiplicity of 2) at a breakup temperature of $T_b\approx 4$ MeV for $a_B=\epsilon_0=15.77$ MeV (nuclear matter parameters), and at $T_b\approx 3$ MeV for empirical parameter values of a finite nucleus which are $a_B=\epsilon_0=8$ MeV. These results are independent of the cutoff temperature T_0 and the size A of the system for a fixed volume [fixed $x(v)$]. The average number of monomers also shows a similar behavior. The average number of monomers $\langle n_1\rangle$ is equal to one at the evaporation temperature of $T_e\approx 6$ MeV for nuclear matter and, for a finite nucleus, $\langle n_1\rangle\approx 1$ at $T_e\approx 4$ MeV. A vaporization temperature T_v, where $A-2$ monomers and only one dimer exist in average with the average multiplicity of $A-1$, is the same for both sets of a_B and ϵ_0 values but depends on the size of the system A and the cutoff temperature T_0. The temperature at which the average energy becomes zero is also insensitive to the cutoff temperature but does depend on the system, i.e., on the size and the parameter values. The average energy is composed of kinetic, binding, and excitation energies. Maximum values of the various fluctuations occur at finite T but depend on the size of the system and the parameter values.

This simple model gives results for the multiplicity distribution which are similar to those in Ref. [12]. We do not have surface effect in contrast to Ref. [12]; we approximate the energy of a cluster to be the form of Eq. (82). The mean multiplicity of Eq. (51) and its fluctuation [cf. Eq. (53)] for $A=100$ with $a_B=\epsilon_0=T_0=15.77$ MeV (Table I) are quite similar to those in Ref. [12] at $T=10$ MeV but somewhat too small at $T=5$ MeV (see Fig. 3). Instead of $\rho_0/\rho=3$, the choice of $\rho_0/\rho=5$, i.e., the two times larger $X_0(T)$ value, was required to obtain a similar result at $T=5$ MeV. This change of the ρ_0/ρ value depicts the lower breakup density (larger fragmentation volume) at lower temperature.

D. Spinodal instability and fragmentation

A thermally equilibrated hot dense system expands until it breaks up due to a spinodal instability $(dP/dV|_T>0)$ [14] or a hydrodynamic instability $(dP/dV|_S>0)$ [15]. On the other hand, as a hot gas system cools down, various sizes of clusters appear through condensation in the spinodal instability region. Figure 4(a) shows the equation of state, i.e., the pressure P vs the density ρ at various temperatures (dotted lines). The results were generated for the single particle mean field energy given by

$$\mathcal{E}(\rho,p)=\frac{p^2}{2M_B}+C_1\rho+C_2\rho^\sigma , \tag{97}$$

and for a phase space distribution given by

$$f(\rho,p)=\frac{1}{\exp[\mathcal{E}(\rho,p)-\mu]/T+1} ,$$
$$\rho=\frac{4}{h^3}\int d^3p\, f(\rho,p) . \tag{98}$$

The self-consistent calculation of Eqs. (97) and (98) determines the density ρ and the chemical potential μ at a given temperature T [16]. The pressure is then given by

$$P=\frac{4}{h^3}\int d^3p\frac{p^2}{3M_B}f(\rho,p)+\frac{1}{2}C_1\rho^2+\frac{\sigma}{\sigma+1}C_2\rho^{\sigma+1} . \tag{99}$$

We choose $C_1=-816.75$ MeV fm^3 and $C_2=3238.1$ MeV fm^6 with $\sigma=2$ which has a nuclear matter saturation density of $\rho_0=0.145$ fm^{-3} with binding energy $E/A=-15.77$ MeV and compressibility of 368 MeV [17]. The compressibility is too high for this parameter set, but our calculations are insensitive to this value. We use the equation of state only to decide the breakup density. From the density dependence of the pressure and the chemical potentials at each temperature, we can determine the spinodal and coexistence lines. These quantities are shown in Fig 4. Here the critical temperature is $T_c=20.95$ MeV with the critical density of $\rho_c=0.3927\rho_0$. Notice also that, at $T=5$ MeV, the upper

TABLE I. Various special temperatures in MeV for nuclear matter values and for empirical values of a_B and ϵ_0 with various cutoff temperature T_0. Here the breakup density appearing in Eq. (96) is set to $A(\rho_0/\rho-1)=200$ which corresponds to fixing $x(v)=1.31$. Temperatures in the row of $\langle M\rangle=2$ are the breakup temperatures T_b at which there are two fragments on average. Temperatures in the row $\langle M\rangle=A-1$ are the vaporization temperatures T_v from which there are no bound nucleons on average. The $(\Delta M)_{\max}$ row shows the temperatures at which the fluctuation in multiplicity is maximum. Total average energy is zero at temperature given in the row of $\langle E\rangle=0$ and the changing rate of energy (heat capacity) is maximum at the temperature in the row of $(\Delta E)_{\max}$. There is one free nucleon on average at the evaporation temperature T_e with $\langle n_1\rangle=1$ and its maximum fluctuation is at temperature in the row of $(\Delta n_1)_{\max}$. In the rows for $\langle M\rangle$ and ΔM at $T=5$ are the multiplicity and its fluctuation, respectively, at temperature $T=5$ MeV. In the rows for $\langle M\rangle$ and ΔM at $T=10$ are the multiplicity and its fluctuation, respectively, at temperature $T=10$ MeV.

$a_B=\epsilon_0$ (MeV)		15.77			8.0	
T_0 (MeV)	0.0	15.77	20.95	0.0	8.0	10.0
	$A=50$					
$\langle M\rangle=2$	4.1	4.3	4.3	2.5	2.7	2.7
$\langle M\rangle=49$	104	185	220	100	185	214
$(\Delta M)_{\max}$	14.0	17.7	18.1	11.0	14.9	15.5
$\langle E\rangle=0$	12.3	12.9	12.8	8.2	8.4	8.4
$(\Delta E)_{\max}$	12.2	13.1	12.6	11.0	22.3	32.5
$\langle n_1\rangle=1$	5.6	5.9	6.0	3.7	4.0	4.0
$(\Delta n_1)_{\max}$	22.3	30.0	32.7	18.3	28.1	30.9
$\langle M\rangle$ at $T=5$	3.35	2.91	2.88	9.03	7.07	6.92
ΔM at $T=5$	2.03	1.69	1.67	5.69	4.55	4.46
$\langle M\rangle$ at $T=10$	16.9	13.6	13.3	24.6	19.0	18.3
ΔM at $T=10$	9.08	7.88	7.74	10.6	9.67	9.50
	$A=100$					
$\langle M\rangle=2$	4.0	4.1	4.1	2.5	2.6	2.6
$\langle M\rangle=99$	250	466	544	246	471	545
$(\Delta M)_{\max}$	18.9	24.6	26.3	15.0	22.3	23.9
$\langle E\rangle=0$	14.9	15.5	15.3	10.0	10.3	10.0
$(\Delta E)_{\max}$	17.7	23.8	20.2	19.6	60.0	83.9
$\langle n_1\rangle=1$	5.6	5.9	6.0	3.7	4.0	4.0
$(\Delta n_1)_{\max}$	31.0	45.7	50.3	27.2	44.2	78.7
$\langle M\rangle$ at $T=5$	3.79	3.25	3.22	11.0	8.43	8.24
ΔM at $T=5$	2.46	2.02	2.00	7.58	5.88	5.75
$\langle M\rangle$ at $T=10$	22.2	17.3	16.9	34.9	25.4	24.4
ΔM at $T=10$	13.8	11.3	11.1	18.7	15.3	14.8

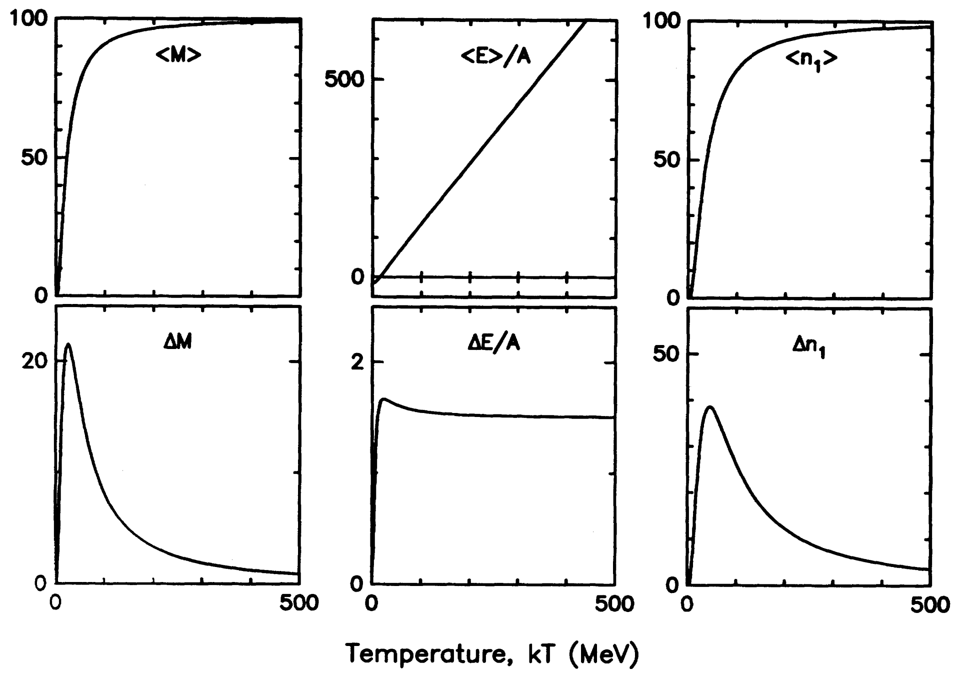

FIG. 2. Temperature dependence of averages and fluctuations of the multiplicity, the total energy in MeV, and the number of monomers for a system with $A=100$ nucleons. $\Delta E = d\langle E\rangle/dT$ which is the heat capacity. Here $y=1$, i.e., x model as in Ref. [1] and the temperature dependences are given by Eqs. (86) and (87) with $a_B=\epsilon_0=T_0=15.77$ MeV and $\rho_0/\rho=3$ for Eq. (96).

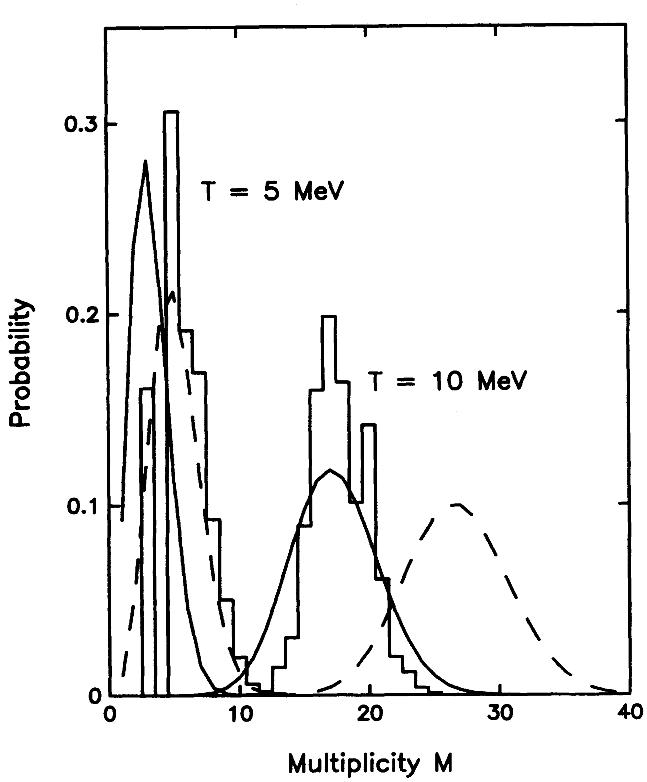

FIG. 3. Multiplicity distribution Eq. (52) in x model of Table I for $A=100$ system at $T=5$ and 10 MeV. The solid lines are with $\rho_0/\rho=3$ and the dashed lines are with $\rho_0/\rho=5$. The histograms are the Monte Carlo calculations of Ref. [12].

density of the spinodal point is $0.6695\rho_0$ and the upper density of the coexist point is $0.9709\rho_0$. At $T=10$ MeV, the upper densities of the spinodal and coexist points are $0.6389\rho_0$ and $0.8887\rho_0$, respectively. The chemical potential μ becomes the same as that for the coexist points at the density ρ/ρ_0 of 0.3568 at $T=5$ MeV and 0.3707 at $T=10$ MeV compared to $\rho_0/3$ which has been used for Table I and Figs. 2 and 3. The densities which correspond to $X_0(T)=1$ and 2 of Eq. (87) with Eq. (96) also are shown in Fig. 4(c). These curves show that the larger system may break up at the higher density for the same temperature.

Figure 5 shows the average and the fluctuation of various thermodynamic quantities along the higher density side of the coexist and spinodal curves. Here we consider a system which can be described with the energy given by Eq. (85) without using a backshifted binding energy in contrast to the case of Table I and Fig. 2. Notice that X_0 becomes large at low density, i.e., at higher T in Fig. 5. This case also shows that the system breaks up into more pieces as the temperature T or the excitation energy becomes higher. At a given temperature (isothermal) [14] or at a fixed entropy (isentropic) [15], the system expands with uniform density until it hits the coexistence or spinodal point. Then the system will break into pieces at some density in either the coexistence or spinodal region at the given temperature T for the isothermal case or at a given entropy for the isentropic case. The coexist and spinodal points at a given T for a given A in Fig. 5 give two different values for each quantity. The actual average and fluctuation for primary fragmentations may be

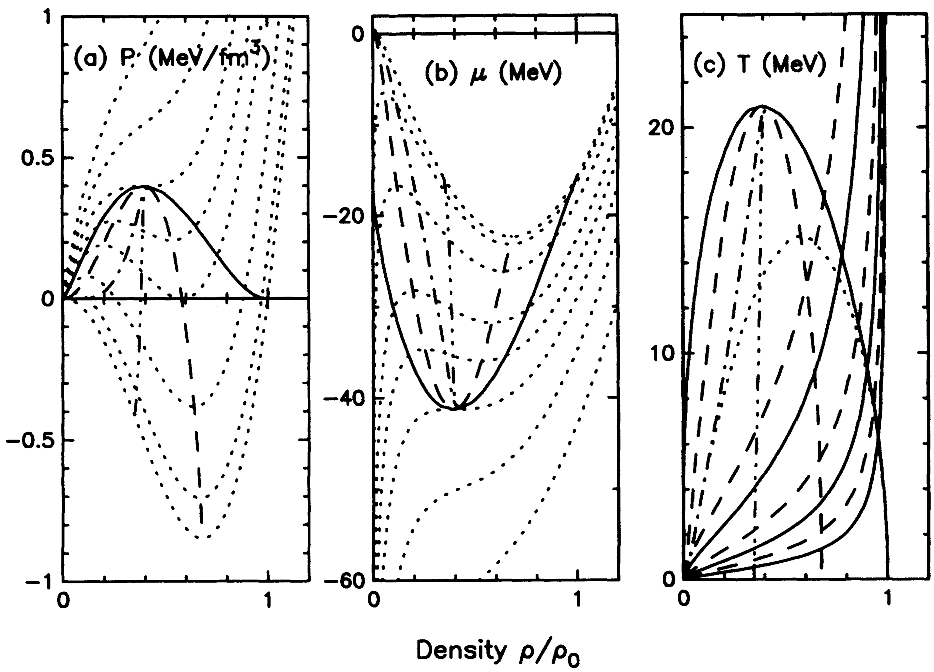

FIG. 4. (a) Equation of state ($P-\rho$) for nuclear matter with BKN force parameters [17] at various temperatures (dotted line). Each dotted line represents the density dependence of the pressure at a temperature T of 0 MeV, 5 MeV, 10 MeV, 15.16 MeV (at which the minimum pressure is 0), 18 MeV, 20.95 MeV [which is the critical temperature T_c (read from bottom up)] 25 MeV, and 30 MeV. (b) The density dependence of the chemical potential μ at various temperatures (dotted line). The temperatures are the same as in (a) but starting from the top. In both (a) and (b), the solid curve is for the coexistent line and the dashed curve is for the spinodal line. The dash-dotted (dash-dot-dot-dotted) line indicate the densities with the same pressure P (chemical potential μ) as the coexistent line at each temperature. (c) The density dependence of the temperatures on the lines mentioned above. The dotted line in (c) is for the density with zero pressure for a given temperature. Here the densities for $X_0(T)=1$ [$X_0(T)=2$] of Eq. (87) with Eq. (96) are also shown as solid (dashed) lines for, from top to bottom, $A=10$, 50, and 200.

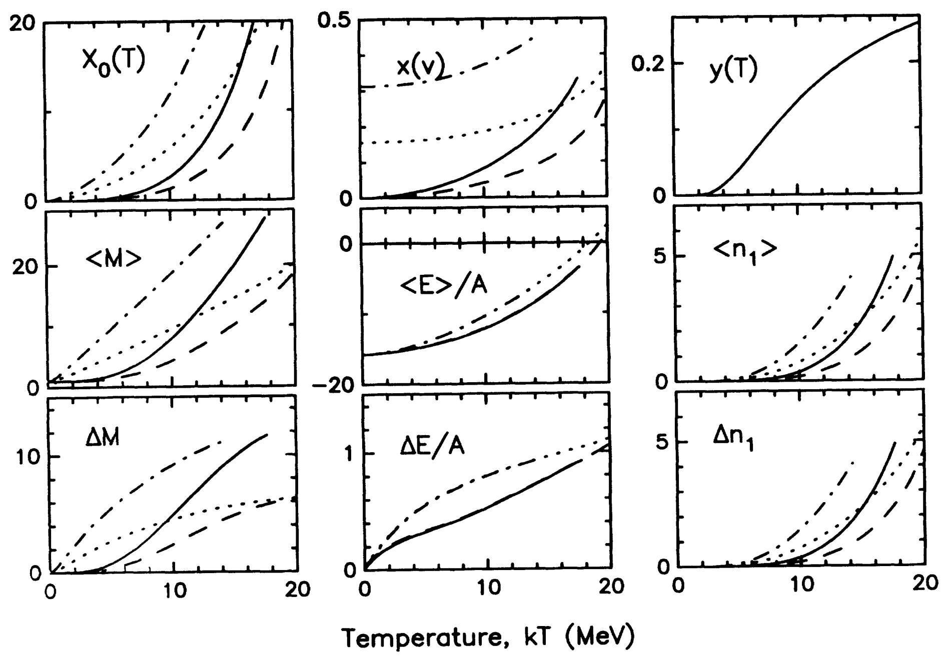

FIG. 5. Temperature dependence of various thermal quantities along the coexistence curve (solid or dashed line) and the spinodal curve (dotted or dash-dotted line) for the densities appearing in the volume dependence factor $x(v)$ of Eq. (96). Here $\Delta E = d\langle E\rangle/dT$ is the heat capacity. Solid and dash-dotted lines are for $A=100$ and dashed and dotted lines are for $A=50$ nucleons.

some value between these two values depending on what density the system breaks up at. The multiplicity and the number of monomers vary widely. These quantities depend on the density at which the system fragments through $X_0(T)=x(v)T^{3/2}$. The average energy is quite insensitive to the fragmentation point. The real empirical results may correspond to much smaller density due to secondary fragmentations. However, due to the finiteness of A for a finite nucleus, the thermodynamic limit is not applicable and the fluctuation effects become important in contrast to the nuclear matter case. Thus there are no clear spinodal and coexistence points. Even the breakup density of a finite nucleus may vary event by event.

Figure 6 shows the cluster size distribution for an $A=50$ system with the energy given by Eq. (85) at $T=5$ and 20 MeV for various breakup densities. It could be a U-shape curve or it could follow a power law depending on the breakup density. If $X_0(T)$ is large due to the low density or high temperature, the size distributions show the power law $k^{-\tau}$ with $\tau\approx 3$ up to $k\approx 10$ and much larger for larger clusters; see the dash-dotted line in Fig. 6(a) and the curves shown in Figs. 6(b) and 6(c) for $T=20$ MeV$\approx T_c$ or 25 MeV. Experimentally τ ranges from 2 to 3 [5,18]. This figure shows the temperature T (or collision energy) dependence of the critical exponent τ [19].

E. Distribution of fragments in a heavy-ion collision

As an application of our simple model to a physical system, Fig. 7 shows the cluster size distribution in Ne+Au$\rightarrow k+X$ reaction at the beam energy of 250 MeV per nucleon [20]. This figure shows a good fit to the data even though we have neglected the surface energy [cf. Eq. (82) or (85)]. For this reaction, our result (long dashed line) with the coexist density at $T=8$ MeV is clearly better than the Bose-Einstein-like distribution Eq. (13) (dash-dot-dot-dotted line) considered in Refs. [5,6] which does not allow the rearrangement of nucleons [weight function $W_A(\mathbf{n},x)=1$ in Eq. (6) in this case]. Here we have taken the number of participant nucleons to be $A=200$. Equation (13) is similar to the dash-dotted line which is our model with the spinodal density at $T=8$ MeV and is good only for small clusters. Equation (13) can become similar to our result (dashed line) only when we take $A=50\,000$ (dotted line). If we take $T=7$ MeV, our model with the density taken to be the higher side of the spinodal density gives a quite similar result as the dash-dot-dot-dotted line [Eq. (13) with $A=200$] and with the higher side of the coexist density gives the same result as the dotted line [Eq. (13) with $A=50\,000$].

Notice that the size distribution is insensitive to the value of y [2] and thus it is determined through the value of $X_0(T)$. The corresponding $X_0(T)$ values are 2.33, 15.67, 1.45, and 12.48 for the dashed line, dash-dotted, dotted, and dash-dot-dot-dotted lines, respectively. These $X_0(T)$ values depend on the values of the number A of participant nucleons, the temperature T, and the breakup density ρ. These parameters should be fitted to obtain better agreement with data.

The fact that our model having the MB-like microstate counting rule for each partition of A nucleons fits the

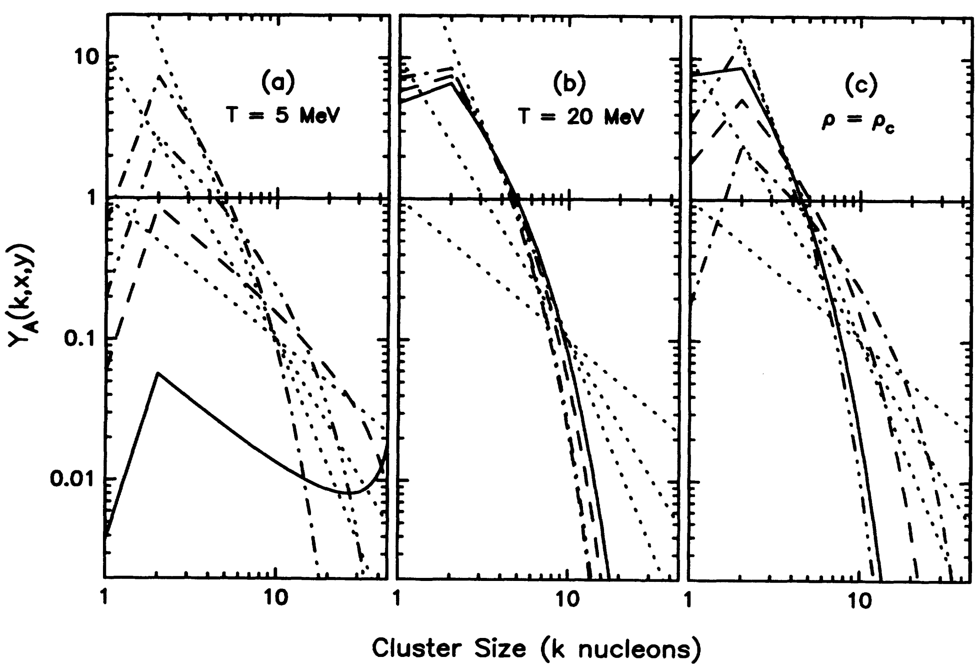

FIG. 6. Cluster size distributions for various cases in a fragmentation of $A=50$ nucleus. (a), (b) The solid curves are with the densities of the coexistence points at the corresponding temperature ($T=5$ and 20 MeV) and the dashed curves are with the densities of the spinodal points. The dash-dotted (dash-dot-dot-dotted) curves are with the densities where the pressure (chemical potential) is the same as the coexistence curve. (c) The critical density ($\rho_c=0.3927\rho_0$). Here the dash-dotted line is at $T=5$ MeV, dashed line is at $T=10$ MeV, solid line is at $T=T_c=20.95$ MeV, and dash-dot-dot-dotted line is at $T=25$ MeV. Dotted lines in these figures show the simple power law, i.e., k^{-1}, $10k^{-2}$, and $100k^{-3}$ and these lines can be compared with the other lines.

data better than Eq. (13) having the BE-like microstate counting rule for each partition of an integer A (see Sec. II B) indicates that the reaction we have considered achieves a uniform thermal system, such as hot nuclear matter or a fireball, before its final breakup into fragments. Fits using the simple form for the energy given by Eq. (82) may indicate that a proper statistical treatment is a more important factor than the details of the interactions between nucleons in the system in describing the fragmentation process at this energy.

V. CONCLUSION

In this paper, fragmentation processes in hadronic collisions are discussed in a unified way using generalized canonical partition functions. The generating function Eq. (14) (grand canonical partition function) of a canonical partition function Eq. (21) with fixed nucleon number A is expressed in terms of a simple multinomial. The average and correlation values of various factorial moments are expressed as simple ratios of this canonical partition function [Eqs. (42) and (43)]. Depending on the choice of the multinomial variable, the model becomes exactly soluble and applicable to various systems as discussed in Ref. [3].

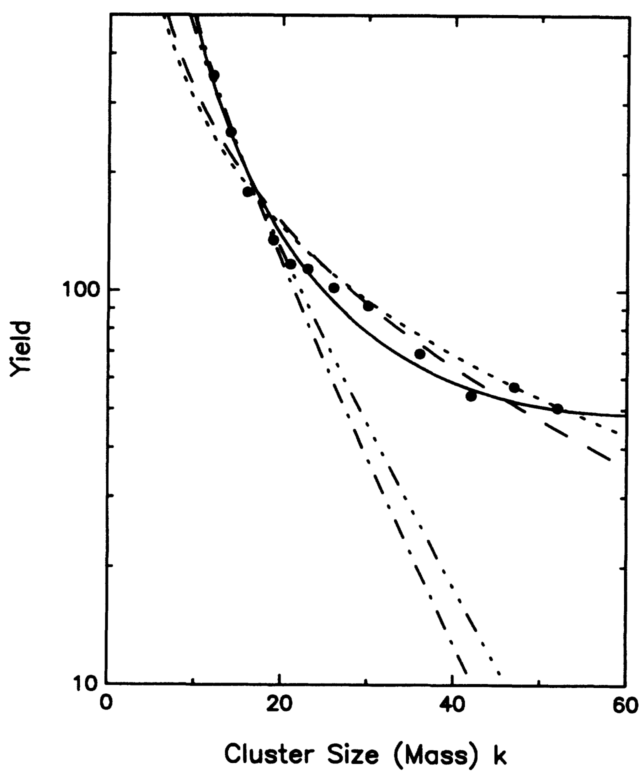

FIG. 7. Mass distribution in Ne+Au→$k+X$ reactions at the beam energy of 250 MeV per nucleon. The filled circles are the data [20] and the solid line is the fit of Ref. [21] with $T=16$ MeV which has the surface energy effect also. The long dashed (dash-dotted) line is our x-y model with the coexist (spinodal) density at $T=8$ MeV and $A=200$ (here $a_B=\epsilon_0=T_0=15.77$ MeV). Our model with spinodal density at $T=7$ MeV is quite similar to the Bose-Einstein-like distribution of Eq. (13) with $A=200$ which is shown by the dash-dot-dot-dotted line. Our model with coexist density at $T=7$ MeV is almost the same as the Bose-Einstein-like distribution of Eq. (13) with $A=50\,000$ which is shown by the dotted line.

Parametrizing the multinomial variables in terms of time or temperature, we also can study the evolution of the system in a clusterization or fragmentation space [Eqs. (59) and (68)]. A general result for the evolution of the system can be reduced to the Fokker-Planck equation, Eq. (77), or the dynamic equation for the multiplicity distribution function of jet fragmentation in ϕ^3 theory [Eq. (61)].

Identifying the multinomial variable as the partition function of the cluster [Eqs. (79) and (86)], we can use the model to study the thermodynamical behavior of a fragmentation process. This study shows there are various types of special temperatures (Table I), such as the breakup temperature T_b at which the system breaks up into two pieces in average, the evaporation temperature T_e having one monomer in average, the vaporization temperature T_v for a total fragmentation, and the temperatures where the average total energy is zero, where the fluctuation becomes maximum, etc. We also have shown that there is U shape or power law in the cluster size distribution depending on the temperature of the system and the volume when the fragmentation occurs (Fig. 6). With this simple model, we were able to fit the nucleus-nucleus collision data (Fig. 7). Further comparison with various reactions will be published elsewhere.

Here we considered only statistics based on Maxwell-Boltzmann-like counting. Bose-Einstein or Fermi-Dirac statistics also can be considered. Also extending the case considered here to various other types of constituents such as quark-gluon would be an interesting problem.

This work was supported in part by National Science Foundation Grant No. 89-03457, by Rutgers University and by the Department of Energy.

APPENDIX A: PARTITION FUNCTIONS FOR $\alpha_i=\beta_i=1$ CASE

For the special case $\alpha_i=\beta_i=1$, the partition functions of Eqs. (14)–(21) are

$$
\begin{aligned}
Q(u,\mathbf{x})&=\exp\left[\left[\sum_{i=1}^{N} x_i\right]u\right] ,\\
A&=\sum_{i=1}^{N}\alpha_i n_i=\sum_{i=1}^{N} n_i=M ,\\
G_A(\mathbf{n},\mathbf{x})&=A!\prod_{i=1}^{N}\left[\frac{x_i^{n_i}}{n_i!}\right] ,\\
Q_A(\mathbf{x})&=\left[\sum_{i=1}^{N}x_i\right]^A .
\end{aligned}
\tag{A1}
$$

For this case, A is same as the multiplicity M and $Q_A=Q_A^M$ is the Ath-order multinomial having the multinomial expansion terms G_A. The average and fluctuations for this case are, from Eqs. (A1) and (42)–(46)

$$Y_A^m(k,\mathbf{x})=[x_k]^m\frac{A!}{(A-m)!}\frac{\left[\sum_i x_i\right]^{A-m}}{\left[\sum_i x_i\right]^A}=\frac{A!}{(A-m)!}\left[\frac{x_k}{\sum_i x_i}\right]^m ,$$

$$\langle n_k n_j\rangle(\mathbf{x})=x_k x_j\frac{A!}{(A-2)!}\frac{\left[\sum_i x_i\right]^{A-2}}{\left[\sum_i x_i\right]^A}=A(A-1)\left[\frac{x_k}{\sum_i x_i}\right]\left[\frac{x_j}{\sum_i x_i}\right] ,$$

$$[\langle n_k^2\rangle-\langle n_k\rangle^2](\mathbf{x})=A(A-1)\left[\frac{x_k}{\sum_i x_i}\right]^2+A\left[\frac{x_k}{\sum_i x_i}\right]-A^2\left[\frac{x_k}{\sum_i x_i}\right]^2 \tag{A2}$$

$$=A\left\{\left[\frac{x_k}{\sum_i x_i}\right]-\left[\frac{x_k}{\sum_i x_i}\right]^2\right\} .$$

These results are obvious from the fact that the corresponding canonical partition function Q_A is just a multinomial of order A.

APPENDIX B: PARTITION FUNCTIONS FOR $\alpha_i=\beta_i=i$ CASE

For $\alpha_i=\beta_i=i$, the partition functions of Eqs. (14)–(22) are

$$Q(u,\mathbf{x})=\exp\left\{\left[\sum_{i=1}^{N}\frac{u^i}{i}x_i\right]\right\} ,$$

$$A=\sum_{i=1}^{N}\alpha_i n_i=\sum_{i=1}^{N} i n_i ,$$

$$G_A(\mathbf{n},\mathbf{x})=A!\prod_{i=1}^{N}\left[\frac{x_i^{n_i}}{i^{n_i}n_i!}\right] , \tag{B1}$$

$$Q_A(\mathbf{x})=\sum_{\{n_i\}_A}G_A(\mathbf{n},\mathbf{x})=\sum_{\{n_i\}_A}A!\prod_{i=1}^{N}\left[\frac{x_i^{n_i}}{i^{n_i}n_i!}\right] ,$$

$$Q_A^M(\mathbf{x})=\sum_{\{n_i\}_{A,M}}A!\prod_{i=1}^{N}\left[\frac{x_i^{n_i}}{i^{n_i}n_i!}\right] .$$

Through the change of variable of $x_i\to ix_i$, this $\alpha_i=\beta_i=i$ case becomes obviously the case of $\alpha_i=i$ and $\beta_i=1$. For $N=\infty$ or $N=A$, Eqs. (B1) reduce to the cases studied in Ref. [1] with $x_i=x$ and in Ref. [2] with $x_i=xy^{\delta_{i,1}}$. Specifically, for $x_i=x$ for all i, using Eqs. (14), (21), and (25), we have

$$Q(u,x)=Q(u,\{x_i=x\})=\exp\left[\sum_{i=1}^{\infty}\frac{xu^i}{i}\right]=\left[\frac{1}{1-u}\right]^x ,$$

$$Q_A(x)=Q_A(\{x_i=x\})=x(x+1)(x+2)\cdots(x+A-1)=\frac{\Gamma(x+A)}{\Gamma(x)} , \tag{B2}$$

$$Q_A^M(x)=Q_A^M(\{x_i=x\})=\frac{1}{M!}\left[\left[\frac{d}{dx}\right]^M Q_A(\{x_i=x\})\right]_{x=0} x^M=(-1)^{A-M}S_A^M x^M ,$$

where $\Gamma(x)$ is the gamma function and S_A^M is the Stirling number [1,4]. This is the case which has been considered in Ref. [1] with A the particle number and M the multiplicity of clusters. For $x_1=xy$ and $x_i=x$ for $i\geq 2$,

$$Q(u,x,y)=Q(u,\{x_i=xy^{\delta_{i,1}}\})=\exp\left[\left[\sum_{i=1}^{\infty}\frac{xu^i}{i}\right]+[x(y-1)u]\right]=\left[\frac{1}{1-u}\right]^x e^{x(y-1)u},$$
$$Q_A(x,y)=Q_A(\{x_i=xy^{\delta_{i,1}}\})=\sum_{r=0}^{A}\frac{A!}{r!(A-r)!}\frac{\Gamma(x+r)}{\Gamma(x)}[x(y-1)]^{A-r}, \tag{B3}$$
$$Q_A^M(x,y)=Q_A^M(\{x_i=xy^{\delta_{i,1}}\})=\frac{1}{M!}\left[\left[\frac{d}{dx}\right]^M Q_A(\{x_i=xy^{\delta_{i,1}}\})\right]_{x=0}x^M.$$

This is the case with two parameters studied in detail in Ref. [2]. Other various choices of x_i's, which also are exactly soluble, are studied in Ref. [3].

For two variables of Eq. (B3), i.e., $x_1=xy$ and $x_i=x$ for $i\geq 2$, the average factorial moments are

$$Y_A^m(k,x,y)=\left\langle\frac{n_k!}{(n_k-m)!}\right\rangle=\left[\frac{xy^{\delta_{k,1}}}{k}\right]^m\frac{A!}{(A-mk)!}\frac{Q_{(A-mk)}(x,y)}{Q_A(x,y)}. \tag{B4}$$

Here $Q_A(x,y)$ is the canonical partition function in the x-y model given in Eq. (B3). When $y=1$, the x-y model becomes the x model of Eq. (B2) and $y=0$ means there are no free nucleons. The detail properties and the various limiting forms of this distribution are discussed in Ref. [2]. We can also easily find the correlations and the fluctuations using Eqs. (45) and (46) for this two-variable case:

$$\langle n_k n_j\rangle=\left[\frac{xy^{\delta_{k,1}}}{k}\right]\left[\frac{xy^{\delta_{j,1}}}{j}\right]\frac{A!}{(A-k-j)!}\frac{Q_{(A-k-j)}(x,y)}{Q_A(x,y)},$$
$$\langle n_k^2\rangle-\langle n_k\rangle^2=\left[\frac{xy^{\delta_{k,1}}}{k}\right]^2\frac{A!}{(A-2k)!}\frac{Q_{(A-2k)}(x,y)}{Q_A(x,y)} \tag{B5}$$
$$+\left[\frac{xy^{\delta_{k,1}}}{k}\right]\frac{A!}{(A-k)!}\frac{Q_{(A-k)}(x,y)}{Q_A(x,y)}-\left[\frac{xy^{\delta_{k,1}}}{k}\right]^2\left[\frac{A!}{(A-k)!}\frac{Q_{(A-k)}(x,y)}{Q_A(x,y)}\right]^2.$$

Since $\langle n_k n_j\rangle$ is exactly the same as Eq. (B4) with $m=1$ except for replacing k by $k+j$ and for an extra factor $[xy^{\delta_{j,1}}/j]$, all the asymptotic forms for Y_A^1 apply to this correlation also.

APPENDIX C: MULTIPLICITY AND ITS FLUCTUATION IN THE x-y MODEL

For $\alpha_i=\beta_i=i$ and $x_i=xy^{\delta_{i,1}}$, i.e., in the x-y model, the mean multiplicity Eq. (51), is, from Eq. (57),

$$\mathcal{M}_A(x,y)=\langle M\rangle=\left[t\frac{d}{dt}\right]\ln Q_A(t\mathbf{x})\bigg|_{t=1}=\left[x\frac{d}{dx}\right]\ln Q_A(x,y)$$
$$=A[x(y-1)]\frac{Q_{(A-1)}(x,y)}{Q_A(x,y)}+\frac{1}{Q_A(x,y)}\sum_{r=1}^{A}x\left[\sum_{p=0}^{r-1}\frac{1}{x+p}\right]\frac{A!}{r!(A-r)!}\frac{\Gamma(x+r)}{\Gamma(x)}[x(y-1)]^{A-r}. \tag{C1}$$

Here $Q_A(x,y)$ is given by Eq. (B3) in Appendix B. The fluctuation of the multiplicity is, from Eq. (58),

$$\Delta\mathcal{M}_A(x,y)=[\langle M^2\rangle-\langle M\rangle^2]=\left[t\frac{d}{dt}\right]^2\ln Q_A(t\mathbf{x})\bigg|_{t=1}=\left[x\frac{d}{dx}\right]^2\ln Q_A(x,y)$$
$$=\left[x\frac{d}{dx}\right]\mathcal{M}_A(x,y)=[\langle M\rangle-\langle M\rangle^2]+\frac{1}{Q_A(X_0,y)}X_0^2\left[\frac{d}{dX_0}\right]^2Q_A(X_0,y)$$
$$=[\mathcal{M}_A(x,y)-\mathcal{M}_A^2(x,y)]+A[x(y-1)]\frac{Q_{A-1}(x,y)}{Q_A(x,y)}\mathcal{M}_{A-1}(x,y)$$
$$+\frac{A[x(y-1)]}{Q_A(x,y)}\sum_{r=1}^{A-1}\left[\sum_{p=0}^{r-1}\frac{x}{x+p}\right]\frac{(A-1)!}{r!(A-1-r)!}\frac{\Gamma(x+r)}{\Gamma(x)}[x(y-1)]^{A-1-r}$$
$$+\frac{1}{Q_A(x,y)}\sum_{r=1}^{A}\left[\left[\sum_{p=0}^{r-1}\frac{x}{x+p}\right]^2-\sum_{p=0}^{r-1}\left[\frac{x}{x+p}\right]^2\right]\frac{A!}{r!(A-r)!}\frac{\Gamma(x+r)}{\Gamma(x)}[x(y-1)]^{A-r}. \tag{C2}$$

These relations are the generalization of Ref. [1] and the detail properties of $\mathcal{M}_A$ and $\Delta\mathcal{M}_A$ are discussed in Ref. [2].

APPENDIX D: DERIVATION OF EQS. (59) AND (64)

Using (34), (39), and (54), we can show that

$$\left[\frac{d}{dt}\right]F^{n_k}_{A,m}(\mathbf{x})=\sum_{j=1}^{N}\left[\frac{d}{dt}\ln x_j(t)\right]\sum_{\{n_i\}_{A,n_k}} n_j\frac{n_k!}{(n_k-m)!}G_A(\mathbf{n},\mathbf{x})$$

$$=\left[\frac{d}{dt}\ln x_k(t)\right]n_kF^{n_k}_{A,m}(\mathbf{x})+\sum_{j\neq k}\left[\frac{d}{dt}\ln x_j(t)\right]\left[\frac{x_j}{\beta_j}\right]\frac{A!}{(A-\alpha_j)!}F^{n_k}_{(A-\alpha_j),m}(\mathbf{x})$$

$$=\frac{A}{\alpha_k}\left[\frac{d}{dt}\ln x_k(t)\right]F^{n_k}_{A,m}(\mathbf{x})$$

$$+\sum_{j=1}^{N}\left[\left[\frac{d}{dt}\right]\ln x_j(t)-\left[\frac{\alpha_j}{\alpha_k}\right]\left[\frac{d}{dt}\right]\ln x_k(t)\right]\left[\frac{x_j}{\beta_j}\right]\frac{A!}{(A-\alpha_j)!}F^{n_k}_{(A-\alpha_j),m}(\mathbf{x})\ . \quad \text{(D1)}$$

Here, in the last equality, we have used the fact that $n_k=[A-\sum_{j\neq k}\alpha_j n_j]/\alpha_k$ due to Eq. (16).

From Eqs. (42), (43), and (59) or (D1),

$$\frac{d}{dt}Y^m_A(k,\mathbf{x})=\frac{\sum_{n_k=0}^{\infty}dF^{n_k}_{A,m}(\mathbf{x})/dt}{Q_A(\mathbf{x})}-\frac{dQ_A(\mathbf{x})/dt}{Q_A(\mathbf{x})}Y^m_A(k,\mathbf{x})$$

$$=\sum_{j=1}^{N}\left[\frac{d}{dt}\ln x_j(t)\right]\left[\left\langle n_j\frac{n_k!}{(n_k-m)!}\right\rangle-\langle n_j\rangle\left\langle\frac{n_k!}{(n_k-m)!}\right\rangle\right]$$

$$=\left[\frac{d}{dt}\ln x_k(t)\right]\left[\left\langle n_k\frac{n_k!}{(n_k-m)!}\right\rangle-Y^1_A(k,\mathbf{x})Y^m_A(k,\mathbf{x})\right]$$

$$+\sum_{j\neq k}^{N}\left[\frac{d}{dt}\ln x_j(t)\right]\left[\frac{x_j}{\beta_j}\right]\frac{A!}{(A-\alpha_j)!}\frac{Q_{(A-\alpha_j)}(\mathbf{x})}{Q_A(\mathbf{x})}[Y^m_{(A-\alpha_j)}(k,\mathbf{x})-Y^m_A(k,\mathbf{x})]$$

$$=\sum_{j=1}^{N}\left[\left[\frac{d}{dt}\right]\ln x_j(t)-\left[\frac{\alpha_j}{\alpha_k}\right]\left[\frac{d}{dt}\right]\ln x_k(t)\right]\left[\frac{x_j}{\beta_j}\right]\frac{A!}{(A-\alpha_j)!}\frac{Q_{(A-\alpha_j)}(\mathbf{x})}{Q_A(\mathbf{x})}$$

$$\times[Y^m_{(A-\alpha_j)}(k,\mathbf{x})-Y^m_A(k,\mathbf{x})]$$

$$=\sum_{j=1}^{N}\left[\left[\frac{d}{dt}\right]\ln x_j(t)-\left[\frac{\alpha_j}{\alpha_k}\right]\left[\frac{d}{dt}\right]\ln x_k(t)\right]Y^{m=1}_A(j,\mathbf{x})[Y^m_{(A-\alpha_j)}(k,\mathbf{x})-Y^m_A(k,\mathbf{x})]\ . \quad \text{(D2)}$$

For the last two relations, Eq. (16) or equivalently the last expression of Eq. (D1) is used.

APPENDIX E: PARTITION FUNCTIONS AND MEAN DISTRIBUTION FOR $x_i=X_0X_1^iy^{\delta_{i,1}}$

For $x_i=X_0X_1^iy^{\delta_{i,1}}$,

$$\sum_{i=1}^{\infty}x_i\frac{u^i}{i}=X_0\sum_{i=1}^{\infty}\frac{(X_1u)^i}{i}+X_0X_1(y-1)u=X_0\ln\left[\frac{1}{1-X_1u}\right]+X_0X_1(y-1)u\ .$$

Thus, from Eqs. (14) and (21), we have

$$Q(u,\{x_i=X_0X_1^iy^{\delta_{i,1}}\})=\left[\frac{1}{1-X_1u}\right]^{X_0}e^{X_0X_1(y-1)u}\ ,$$

$$Q_A(\{x_i=X_0X_1^iy^{\delta_{i,1}}\})=\sum_{r=0}^{A}\frac{A!}{r!(A-r)!}X_1^r\frac{\Gamma(X_0+r)}{\Gamma(X_0)}[X_0X_1(y-1)]^{A-r}=X_1^AQ_A(X_0,y)\ . \quad \text{(E1)}$$

The $Q_A(X_0,y)=Q_A(\{x_i=X_0y^{\delta_{i,1}}\})$ is given by Eq. (B3) in Appendix B with $x=X_0$. The results of Eq. (E1) are of a very simple form and they lead to an exactly soluble model (see below). The average number of clusters [Eq. (44)] is

$$\langle n_k \rangle = \left[\frac{X_0 X_1^k y^{\delta_{k,1}}}{k} \right] \frac{A!}{(A-k)!} \frac{X_1^{A-k} Q_{(A-k)}(X_0,y)}{X_1^A Q_A(X_0,y)} = Y_A^1(k,X_0,y) \ . \tag{E2}$$

This result is the same as Eq. (B4) with $m=1$ and $x_i = xy^{\delta_{i,1}} = X_0 y^{\delta_{i,1}}$ [2]. Similarly, the correlations and the fluctuations are the same as Eq. (B5). Using Eqs. (80) and (81) with $X_0 \to X_0 e^t$ in Eq. (E1), which corresponds to $f_i(t)=1$ in Eq. (79), the average multiplicity and its fluctuation are found to be given by

$$\begin{aligned}\langle M \rangle &= \left[\left[\frac{d}{dt} \right] \ln Q_A(\{x_i = X_0 e^t X_1^i y^{\delta_{i,1}}\}) \right]_{t=0} = \left[X_0 \frac{d}{dX_0} \right] \ln[X_1^A Q_A(X_0,y)] \\ &= \left[X_0 \frac{d}{dX_0} \right] \ln Q_A(X_0,y) = \mathcal{M}_A(X_0,y) \ ,\end{aligned} \tag{E3}$$

$$\begin{aligned}[\langle M^2 \rangle - \langle M \rangle^2] &= \left[\left[\frac{d}{dt} \right]^2 \ln Q_A(\{x_i = X_0 e^t X_1^i y^{\delta_{i,1}}\}) \right]_{t=0} \\ &= \left[X_0 \frac{d}{dX_0} \right]^2 \ln Q_A(X_0,y) = \left[X_0 \frac{d}{dX_0} \right] \mathcal{M}_A(X_0,y) = \Delta\mathcal{M}_A(X_0,y) \ .\end{aligned} \tag{E4}$$

Here $\mathcal{M}_A(X_0,y)$ and $\Delta\mathcal{M}_A(X_0,y)$ are given by Eqs. (C1) and (C2) in Appendix C with $x = X_0$ and these results are the same as the $x_i = xy^{\delta_{i,1}}$ case considered in Ref. [2]. The results of Eqs. (E2)–(E4) are independent of X_1 and that is understandable since the quantity X_1 is the same for every nucleon independent of the cluster to which it belongs and thus cannot affect the clusterization process. For $x_i(t=1/T)$ of Eq. (86), we have $\langle M \rangle = 1$ at $T=0$ and $\langle M \rangle = A$ at $T=\infty$ since $X_0(T) \to 0$ as T goes to zero and $X_0(T) \to \infty$ as the temperature T becomes infinitely large (see Appendix F). Furthermore, the fluctuation in the multiplicity $\Delta\mathcal{M}_A(X_0,y)$ is zero at both $T=0$ and $T=\infty$.

APPENDIX F: ASYMPTOTIC BEHAVIOR AT LOW AND HIGH TEMPERATURES

Asymptotic behaviors of Eq. (87) are

$$\begin{aligned}&X_1(T \approx 0) \approx e^{-(M_B - a_B)/T} \ , \\ &y(T \approx 0) \approx e^{-a_B/T} \ , \\ &X_1(T >> M_B - a_B) \approx \exp\left[\frac{1}{\epsilon_0} \left[\frac{T_0 T}{T + T_0} \right] \right] \approx e^{T_0/\epsilon_0} \ , \\ &y(T >> a_B) \approx \exp\left[-\frac{1}{\epsilon_0} \left[\frac{T_0 T}{T + T_0} \right] \right] \approx e^{-T_0/\epsilon_0} \ .\end{aligned} \tag{F1}$$

All of $X_0(T)$, $X_1(T)$, and $y(T)$ are zero at $T=0$. At high temperature $T \to \infty$, $X_1(T) = \exp(T_0/\epsilon_0)$ and $y(T) = \exp(-T_0/\epsilon_0)$ are finite and $X_0(T) \to \infty$. The asymptotic form [2] of the $Q_A(x,y)$ of Eq. (B3) is

$$Q_A(x,y) \approx Q_A(x) + A[x(y-1)]Q_{A-1}(x) \ , \tag{F2}$$

for $x \approx 0$ or $y \approx 1$, i.e., for $[x(y-1)] \approx 0$ and

$$Q_A(x,y) \approx (xy)^A + \frac{A(A-1)}{2xy^2}(xy)^A \ , \tag{F3}$$

for $x >> A$ since $Q_r(x) = \Gamma(x+r)/\Gamma(x) \approx x^r + \frac{1}{2} r(r-1) x^{r-1}$. Thus at low and high temperatures, the partition function $Q_A(X_0,y)$ in Eq. (E1) becomes

$$\begin{aligned}&Q_A(X_0,y; T \approx 0) \approx X_0(A-1)! \approx x(v) T^{3/2} (A-1)! \ , \\ &Q_A(X_0,y; T \to \infty) \approx (X_0 y)^A \approx [x(v) T^{3/2} e^{-T_0/\epsilon_0}]^A \ .\end{aligned} \tag{F4}$$

Notice here also that $Q_0(\mathbf{x}) = 1$ in general.

We have the following asymptotic behaviors [2] for the cluster distribution. The asymptotic behavior at low and high temperatures of the average cluster distribution Eq. (E2) are

$$\langle n_k\rangle(T\approx 0)\approx\left[\frac{X_0y^{\delta_{k,1}}}{k}\right]\left[\frac{A}{A-k}\right]\left[\frac{A-k}{X_0}\right]^{\delta_{k,A}}\approx\left[\frac{A}{k}\right]\left[\frac{x(v)T^{3/2}}{A-k}\right]^{1-\delta_{k,A}}e^{-\delta_{k,1}a_B/T},$$
$$\langle n_k\rangle(T\to\infty)\approx\left[\frac{X_0y^{\delta_{k,1}}}{k}\right]\frac{A!}{(A-k)!}\left[\frac{1}{X_0y}\right]^{k}\approx\left[\frac{1}{k}\right]\frac{A!}{(A-k)!}[x(v)T^{3/2}]^{(1-k)}e^{(k-\delta_{k,1})T_0/\epsilon_0},\qquad\text{(F5)}$$

and their fluctuations Eq. (B5) are

$$[\langle n_k^2\rangle-\langle n_k\rangle^2](T\approx 0)\approx\left[\frac{X_0y^{\delta_{k,1}}}{k}\right]^2\left[\frac{A}{A-2k}\right]\left[\frac{A-2k}{X_0}\right]^{\delta_{2k,A}}\theta(A-2k)$$
$$+\left[\frac{X_0y^{\delta_{k,1}}}{k}\right]\left[\frac{A}{A-k}\right]\left[\frac{A-k}{X_0}\right]^{\delta_{k,A}}-\left[\frac{X_0y^{\delta_{k,1}}}{k}\right]^2\left[\frac{A}{A-k}\right]^2\left[\frac{A-k}{X_0}\right]^{2\delta_{k,A}}$$
$$\approx\left[\frac{A}{k}\right]\left[\frac{x(v)T^{3/2}}{A-k}\right]^{1-\delta_{k,A}}e^{-\delta_{k,1}a_B/T}[1-\delta_{k,A}],$$
$$[\langle n_k^2\rangle-\langle n_k\rangle^2](T\to\infty)\approx\left[\frac{X_0y^{\delta_{k,1}}}{k}\right]^2\frac{A!}{(A-2k)!}\left[\frac{1}{X_0y}\right]^{2k}\theta(A-2k)\qquad\text{(F6)}$$
$$+\left[\frac{X_0y^{\delta_{k,1}}}{k}\right]\frac{A!}{(A-k)!}\left[\frac{1}{X_0y}\right]^{k}-\left[\frac{X_0y^{\delta_{k,1}}}{k}\right]^2\left[\frac{A!}{(A-k)!}\right]^2\left[\frac{1}{X_0y}\right]^{2k}$$
$$\approx\left[\frac{1}{k}\right]\frac{A!}{(A-k)!}[x(v)T^{3/2}]^{(1-k)}e^{(k-\delta_{k,1})T_0/\epsilon_0}[1-\delta_{k,1}].$$

The step function $\theta(a)$ is 1 for $a\geq 0$ and is zero otherwise. Thus $\langle n_1\rangle=0$ and $\langle n_A\rangle=1$ at $T=0$, and $\langle n_1\rangle=A$ and $\langle n_A\rangle=0$ at $T=\infty$. The fluctuation becomes zero at both $T=0$ and $T=\infty$.

The asymptotic behavior at low and high temperature for the mean multiplicity of Eq. (E3) are, from Eq. (C1),

$$\langle M\rangle(T\approx 0)\approx 1+\sum_{r=2}^{A}\frac{X_0}{r-1}+\frac{AX_0(y-1)}{(A-1)}\approx 1+x(v)T^{3/2}\sum_{r=2}^{A}\frac{1}{r-1}+\frac{A}{(A-1)}x(v)T^{3/2}[e^{-a_B/T}-1],$$
$$\langle M\rangle(T\approx\infty)\approx A-\frac{A(A-1)}{2X_0y^2}\approx A-\frac{A(A-1)}{2}[x(v)T^{3/2}]^{-1}e^{2T_0/\epsilon_0}.\qquad\text{(F7)}$$

In Eq. (F7), we have retained both terms in Eqs. (F2) and (F3). Since $\Delta\mathcal{M}_A(x,y)=[xd/dx]\mathcal{M}(x,y)$ [Eq. (C2)], we have, for the fluctuation of the multiplicity Eq. (E4),

$$\langle(M-\langle M\rangle)^2\rangle(T\approx 0)\approx\sum_{r=2}^{A}\frac{X_0}{r-1}+\frac{AX_0(y-1)}{(A-1)}\approx x(v)T^{3/2}\sum_{r=2}^{A}\frac{1}{r-1}+\frac{A}{(A-1)}x(v)T^{3/2}[e^{-a_B/T}-1],$$
$$\langle(M-\langle M\rangle)^2\rangle(T\approx\infty)\approx\frac{A(A-1)}{X_0y^2}=\frac{A(A-1)}{2}[x(v)T^{3/2}]^{-1}e^{2T_0/\epsilon_0}.\qquad\text{(F8)}$$

Thus $\langle M\rangle=1$ at $T=0$ ($X_0=0$) and $\langle M\rangle=A$ at $T=\infty$ ($X_0=\infty$). Furthermore, the fluctuation of the multiplicity is zero at both of $T=0$ and $T=\infty$.

---

[1] A. Z. Mekjian, Phys. Rev. C **41**, 2103 (1990); Phys. Rev. Lett. **64**, 2125 (1990).

[2] S. J. Lee and A. Z. Mekjian, Phys. Lett. A **149**, 7 (1990).

[3] A. Z. Mekjian and S. J. Lee, Phys. Rev. A **44**, 6294 (1991).

[4] M. Abramowitz and I. Stegun, *Handbook of Mathematics Functions,* Natl. Bur. Stand. (U.S.) Appl. Math. Series No. 55 (U.S. GPO, Washington, DC, 1965).

[5] J. Aichelin and J. Huefner, Phys. Lett. **136B**, 15 (1984); J. Aichelin, J. Hüfner, and R. Ibarra, Phys. Rev. C **30**, 107 (1984).

[6] L. G. Sobotka and L. G. Moretto, Phys. Rev. C **31**, 668 (1985).

[7] A. J. Cole, Phys. Rev. C **40**, 2024 (1989).
[8] R. C. Hwa, in *Hadronic Matter in Collision 1988*, edited by P. A. Carruthers and J. Rafelski (World Scientific, Singapore, 1989), p. 225; in *Hadronic Multiparticle Production*, edited by P. A. Carruthers (World Scientific, Singapore, 1988), p. 556; Z. Phys. C **38**, 277 (1988).
[9] P. Bak, C. Tang, and K. Wiesenfeld, Phys. Rev. B **38**, 364 (1988); L. P. Kadanoff, S. R. Nagel, L. Wu, and S. Zhou, Phys. Rev. A **39**, 6524 (1989).
[10] E. M. Lifshitz and L. P. Pitaevskii, *Physical Kinetics* (Pergamon, Oxford, 1981).
[11] A. R. DeAngelis and A. Z. Mekjian, Phys. Rev. C **40**, 105 (1989).
[12] J. P. Bondorf *et al.*, Nucl. Phys. **A443**, 321 (1985).
[13] D. H. E. Gross and X. Z. Zhang, Nucl. Phys. **A495**, 231c (1989); J. P. Bondorf *et al.*, *ibid.* **A444**, 460 (1985).
[14] P. Schuck *et al.*, Prog. Part. Nucl. Phys. **22**, 181 (1989).
[15] G. Bertsch and P. J. Siemens, Phys. Lett. **126B**, 9 (1983).
[16] C. Gale, G. M. Welke, M. Prakash, S. J. Lee, and S. Das Gupta, Phys. Rev. C **41**, 1545 (1990).
[17] P. Bonche, S. E. Koonin, and J. W. Negele, Phys. Rev. C **13**, 1226 (1976); S. J. Lee, H. H. Gan, E. D. Cooper, and S. Das Gupta, *ibid.* **40**, 2585 (1989).
[18] H.-A. Gustafsson *et al.*, Phys. Lett. B **241**, 322 (1990).
[19] K. K. Gudima and Yu. A. Murin, Phys. Lett. B **234**, 1 (1990).
[20] A. I. Warwick *et al.*, Phys. Rev. C **27**, 1083 (1983).
[21] A. L. Goodman, J. I. Kapusta, and A. Z. Mekjian, Phys. Rev. C **30**, 851 (1984).